

RCU2 testing and design

Inge Nikolai Torsvik



Master Thesis

*Department of Physics and Technology
University of Bergen*

November 2013

Abstract

Contents

Contents

| | | |
|----------|--|-----------|
| 1 | Introduction | 1 |
| 1.1 | How to test | 1 |
| 1.2 | About this work | 2 |
| 2 | ALICE experiment | 3 |
| 2.1 | The Time Projection Chamber TPC | 4 |
| 2.2 | The TPC Front End electronics FEE | 4 |
| 2.2.1 | Front End Card FEC | 5 |
| 2.2.2 | Readout Control Unit RCU | 7 |
| 2.2.3 | RCU2 | 7 |
| 3 | Radiation and Radiation effect on Semiconductor devices | 10 |
| 3.1 | Interaction of Radiation With Matter | 10 |
| 3.2 | Charge particle and their Interaction with Matters | 10 |
| 3.2.1 | Stopping Power | 11 |
| 3.2.2 | Specific Stopping Power | 12 |
| 3.2.3 | Linear Energy Transfer LET | 13 |
| 3.3 | Neutral particle and their Interaction with Matter | 14 |
| 3.3.1 | Neutrons | 14 |

| | | |
|----------|--|-----------|
| 3.3.2 | Photons | 14 |
| 3.4 | Radiation Effects on Semiconductor Devices | 14 |
| 3.4.1 | Single Events Effects SEE | 15 |
| 3.4.2 | Accumulative Effects | 18 |
| 3.4.3 | The TPC radiation environment | 19 |
| 4 | The Test Chips and Preparations for Testing | 20 |
| 4.1 | The Integrated Circuits Which Where Tested | 20 |
| 4.1.1 | TPS51200 | 21 |
| 4.1.2 | MIC69302WU | 21 |
| 4.1.3 | SN74AVCB164245 | 22 |
| 4.1.4 | SN74AVC2T245 | 24 |
| 4.1.5 | QS3VH257 | 24 |
| 4.1.6 | SY89831U | 25 |
| 4.1.7 | ADN2814 and MAX3748 | 27 |
| 4.1.8 | INA210 | 28 |
| 4.1.9 | TLV3011 | 29 |
| 4.1.10 | SmartFusion2 | 32 |
| 4.1.11 | Software | 36 |
| 5 | Testing at Oslo Cyclotron Laboratory (OCL) | 36 |
| 5.1 | About OCL | 36 |

| | | |
|----------|--|-----------|
| 5.2 | Experiment setup and equipment | 37 |
| 5.3 | Measurement equipment and test boards | 39 |
| 5.3.1 | static RAM (SRAM) board | 39 |
| 5.3.2 | Scintillator counter | 41 |
| 5.3.3 | X-Y-positioning system | 42 |
| 5.4 | Preparation and characterization of the beam | 43 |
| 5.4.1 | Purpose of tests | 43 |
| 5.4.2 | Beam setup | 43 |
| 6 | Results and calculations from beam test at OCL | 45 |
| 6.1 | Calibration process | 45 |
| 6.2 | Test results | 45 |
| 6.2.1 | TPS51200 | 48 |
| 6.2.2 | MIC69302WU | 48 |
| 6.2.3 | SN74AVCB164245 | 49 |
| 6.2.4 | SN74AVC2T245 | 49 |
| 6.2.5 | QS3VH257 | 50 |
| 6.2.6 | SY89831 | 51 |
| 6.2.7 | ADN2814 | 51 |
| 6.2.8 | MAX3748 | 53 |
| 6.3 | Calculation of dose | 54 |
| 6.4 | Discussion of the result | 55 |

| | |
|--------------------------|-----------|
| 7 Conclusion | 56 |
| 8 Appendix | 57 |
| 8.1 datasheets | 57 |

| | |
|----------------|---|
| CERN | European Council for Nuclear Research |
| ALICE | A Large Ion Collider Experiment |
| OCL | Oslo Cyclotron Laboratory |
| DUT | Device Under Test |
| RCU | Readout Control Unit |
| RCU2 | Readout Control Unit 2 |
| LHC | Large Hadron Collider |
| FEE | Front End Electronic |
| FEC | Front End Card |
| FPGA | Field Programmable Gate Array |
| SEE | Single Even Effect |
| SEU | Single Event Upset |
| SET | Single Event Transient |
| SEL | Single Event Latchup |
| IC | Integrated Circuit |
| PCB | Printed Circuit Board |
| LVDS | Low-Voltage Differential Signaling |
| DAQ | Data Acquisition |
| SF2 | SmartFusion2 |
| CML | Current-Mode Logic |
| TPC | Time Projection Chamber |
| LVPECL | Low Voltage Positive Emitter Coupled Logic |
| SRAM | static RAM |
| PM-tube | PhotoMultiplier Tube |
| TID | Total Ionizing Dose |
| UART | Universal Asynchronous Receiver/Transmitter |
| ADC | Analog to Digital Converter |
| LET | Linear Energy Transfer |

| | |
|-------------|---|
| SoC | System On a Chip |
| CMOS | Complementary Metal Oxide Semiconductor |
| DCS | Control System board |
| SIU | Source Interface Unit |
| TSL | The Svedberg Laboratory |
| MSS | Microcontroller SubSystem |
| WSR | Windowed Shift Register |

1 Introduction

At European Council for Nuclear Research (CERN) in Switzerland there are being conducted experiment on fundamental structure of the universe. This is done by accelerating particles up to a energy of 4 TeV per proton, and then crash with a other particle with same energy. This experiment is done by connecting several accelerators with higher and higher energies together to accelerate particles. The largest one is called Large Hadron Collider (LHC), and is the largest particle accelerator ever built, installed in a 27 km long tunnel. To detect what is happening to the particles when crashed, there has been built several detectors that is placed in the tunnel. One of these is called A Large Ion Collider Experiment (ALICE). The ALICE detector is built to study a matter known as Quark-gluons plasma [1], which will be generated under collisions of heavy ions. The detector consist of several sub-detector with different functionality. Time Projection Chamber (TPC) is one of these, and is the main tracking detector placed in the inner circle of ALICE, see section 2. Under a collision high energetic neutrons and protons will be generated, and will also pose a risk to the electronics used. It is therefore of highest importance to test everything that are planed to be used in the experiment for radiation. A replacement of electronics after installed in the detector is normally impossible under a run period, which can last up to several years.

One of the main boards used in the TPC detector is the Readout Control Unit (RCU). Now there has been decided that a new RCU board shall be made, namely the Readout Control Unit 2 (RCU2). Everything that are going to be used in the LHC tunnel has to be made sure that it can survive the radiation level that are there. Therefore every Integrated Circuit (IC) planned to be used for the design of the RCU2 board has to be tested for radiation to be sure that it won't fail when it is installed in the TPC detector.

1.1 How to test

The radiation tests done through this thesis is mainly Total Ionizing Dose (TID) test. That is irradiation up to a level where an error can clearly be seen or when a high enough dose has been reached without detecting errors, see section 3.4.2 for more information. But there has also been done tests for Single Event Effect (SEE), like Single Event Upset (SEU), Single Event Transient (SET) and Single Event Latchup (SEL) on a Microsemi SmartFusion2 (SF2) System On a Chip (SoC) Field Programmable Gate Array (FPGA).

1.2 About this work

When I started working with my thesis in the autumn of 2013 the schematic layout for the RCU2 was basically finished, and most of the component was decided, but not all of the component had been tested. My work through this thesis has been planning how to test different circuits, designing test setup and executing the tests. For most of the circuits, I designed a Printed Circuit Board (PCB) with only the necessary to make the circuit work and to be able to test it. By the use of Data Acquisition (DAQ) boards from National Instruments, the PCB was connected to a computer where inputs were controlled and the outputs and current consumption was measured through a labVIEW program. For the more advanced IC like the SF2, I used a starter-kit when designing the test, and wrote test code in VHDL and C. I also made a Printed Circuit Board (PCB) for measuring current and control a power regulator on the SF2 starter-kit. The circuits I have tested consist of: SoC FPGA, power regulators, bus transceivers, limiting amplifier, multiplexer/demultiplexer and buffer, comparator and Current Shunt Monitor. Every test board I made was radiation tested in OCL at the University of Oslo, the SF2 chip was also radiation tested in The Svedberg Laboratory (TSL) in Uppsala in Sweden.

2 ALICE experiment

Since 1954 physicists at CERN have studied the nucleus and its structure to find the fundamental structure of the universe. CERN is the world largest research center for nuclear and particle physics, and has a total of 21 member state. One of the biggest and newest invention at CERN is the Large Hadron Collider (LHC), that is a circular particle accelerator placed in a 27 km long tunnel around 100 meter beneath ground level. This is the last accelerator in a chain of up to 7 (depending on which particle to accelerate), where the particles gradually accelerate to higher and higher energies, up to their maximum energy of 4 TeV and speed up to the speed of light. When particles has reached this energy level accelerated particles from opposite direction are made to collide inside 4 different experiment areas, where one of these is called A Large Ion Collider Experiment (ALICE). See figure 2.1.

The ALICE detector is a heavy ion detector. Its main purpose is to study a state of matter called quark-gluon plasma¹ which will be generated when heavy ions collides. Under a such collision a temperature 100 000 times higher than the temperature of the sun is generated. There is then high enough energy to split the protons and neutrons, and achieve a plasma of unbound quarks and gluons, and that is called quark-gluon plasma.

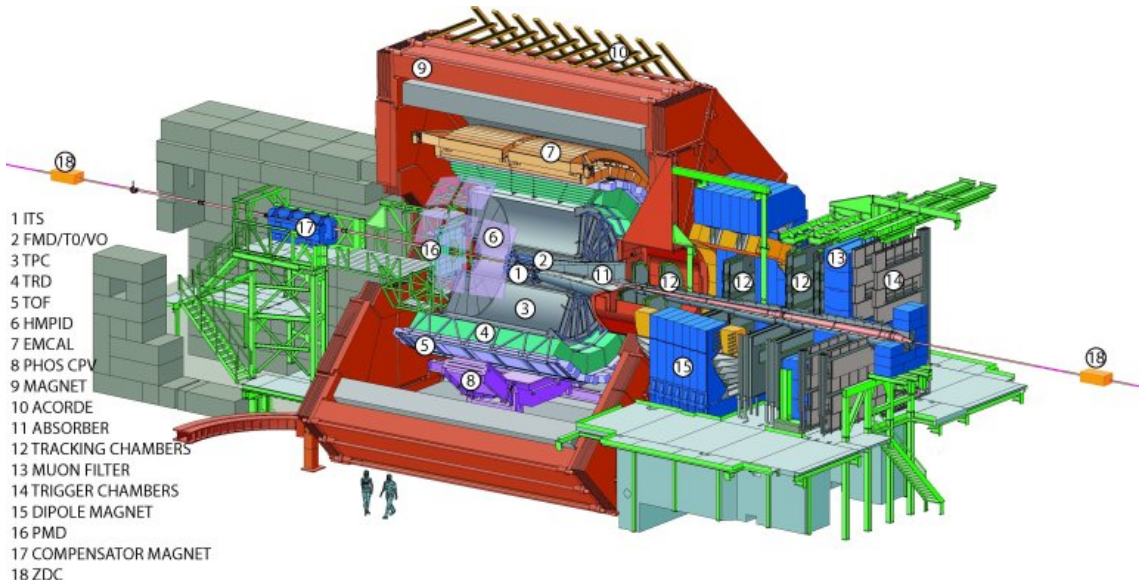


Figure 2.1: Layout of the ALICE experiment [6]

CERN

¹All ordinary matter in today's universe is made up of atoms. Each atom contains a nucleus composed of protons and neutrons (except hydrogen, which has no neutrons), surrounded by a cloud of electrons. Protons and neutrons are in turn made of quarks bound together by other particles called gluons. No quark has ever been observed in isolation: the quarks, as well as the gluons, seem to be bound permanently together and confined inside composite particles, such as protons and neutrons.

2.1 The Time Projection Chamber TPC

The ALICE detector comprises of several sub-detectors, where one of these is the Time Projection Chamber (TPC). TPC is the main tracking detector placed in the inner circle of ALICE. The function of TPC are tracking particles, measure the charged particles momentum and identification of particles. A drawing of the TPC can be seen in figure 2.2. The TPC detector has a cylindrical shape, with a inner radius of 85 cm and outer radius of 250 cm, and has an overall length of 510 cm. The detector is made up of a large cylindrical field cage, filled with 88 m^3 of 90% Ne gas and 10% CO_2 gas. A high voltage electrode is placed in the center of the detector. When a charged particle is generated inside the detector, the gas inside the cage will be ionized and make electrons drift in the electric field between the high voltage electrode and the two end plates. At the end-plates we find the Readout Chamber which are divided into 18 trapezoidal sectors, and each sector is again divided into the inner and outer chamber. In the readout chamber, there are a total of 560 000 readout pads of three different sizes: $4 \times 7.5 \text{ mm}^2$ in the inner chambers, $6 \times 10 \text{ mm}^2$ and $6 \times 15 \text{ mm}^2$ in the outer chambers.

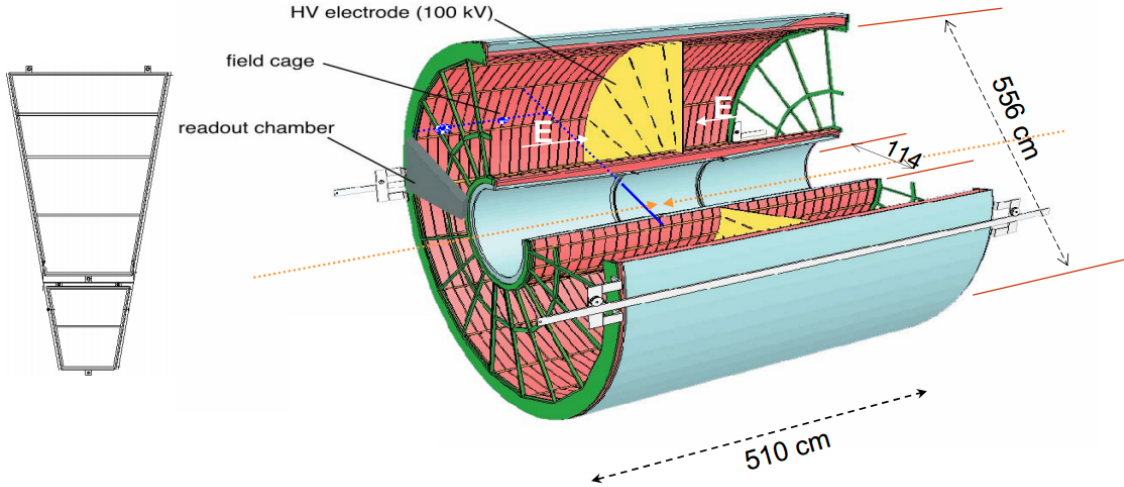


Figure 2.2: Layout of the TPC [6]

2.2 The TPC Front End electronics FEE

Each of the total 36 sections are also divided into 6 readout partitions, that is 2 in the inner chamber and 4 in the outer chamber. Each of the readout partitions are controlled by a Readout Control Unit (RCU) which is connected to 18 to 25 Front End Card (FEC). See figure 2.3 There are a total of 216 RCU connected to a total of 4356 FEC which is connected to all of the 560 000 readout pads, and all together this sums up the Front End Electronic (FEE). In short the task of the FEE is to read out charge received at the readout pads, process it and send useful data to a computer.

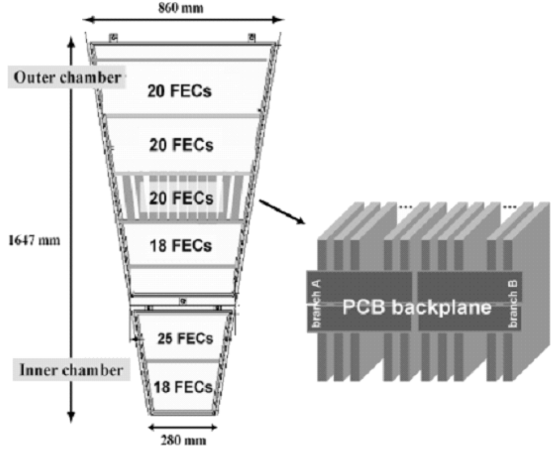


Figure 2.3: A TPC sector. Showing how FEC is placed [13]

2.2.1 Front End Card FEC

When one of the pads receives a charge after a collision has occurred, it sends out a current signal with a rise time of less than 1 ns followed by a long tail due to the motion of the positive ions. The amplitude is slightly different for the different pad sizes, but has a typical value of around $7 \mu\text{A}$. A current signal given by one of the pads, is sent into the Front End Card (FEC) which consist of three basic functional units, see block diagram in figure 2.4. The first unit is a charge sensitive amplifier/shaper called PASA, the second unit is a 10-bit 25MHz low-power Analog to Digital Converter (ADC). The last unit is a digital circuit that perform the baseline subtraction, tail cancellation, zero-suppression², formatting and buffering. The ADC and the digital unit together constitute the so called ALTRO chip. There are 16 PASA chips and 16 ALTRO chips on the FEC, the PASA chip is connected to 16 readout pads each, which gives a total of 128 readout pads for each FEC. An picture of the FEC can be seen in figure 2.5.

²Zero Compressions means that signal bellow a given threshold will be filtered away.

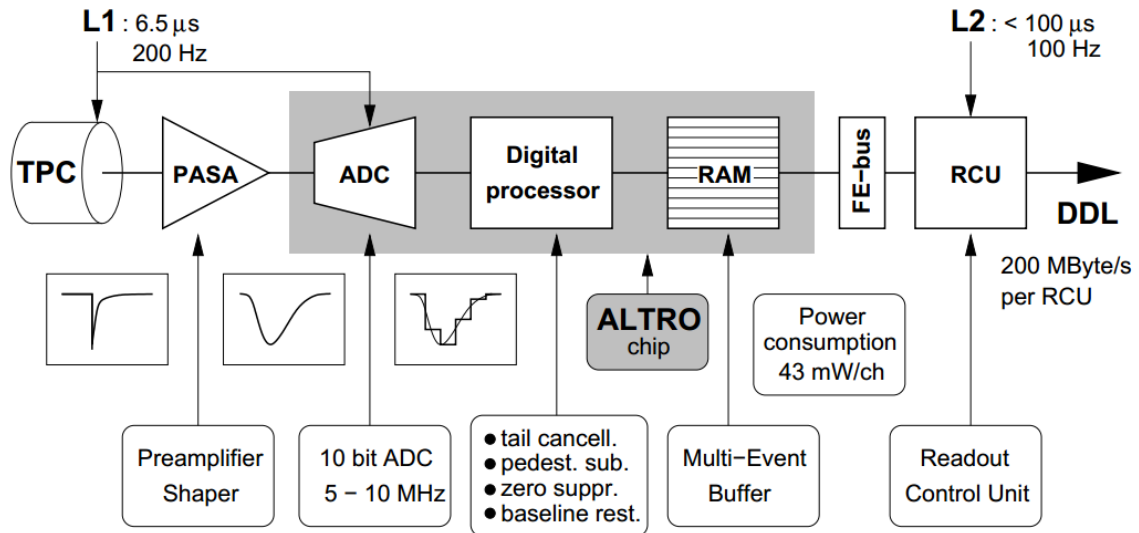


Figure 2.4: Block diagram of the Front End Card [6]

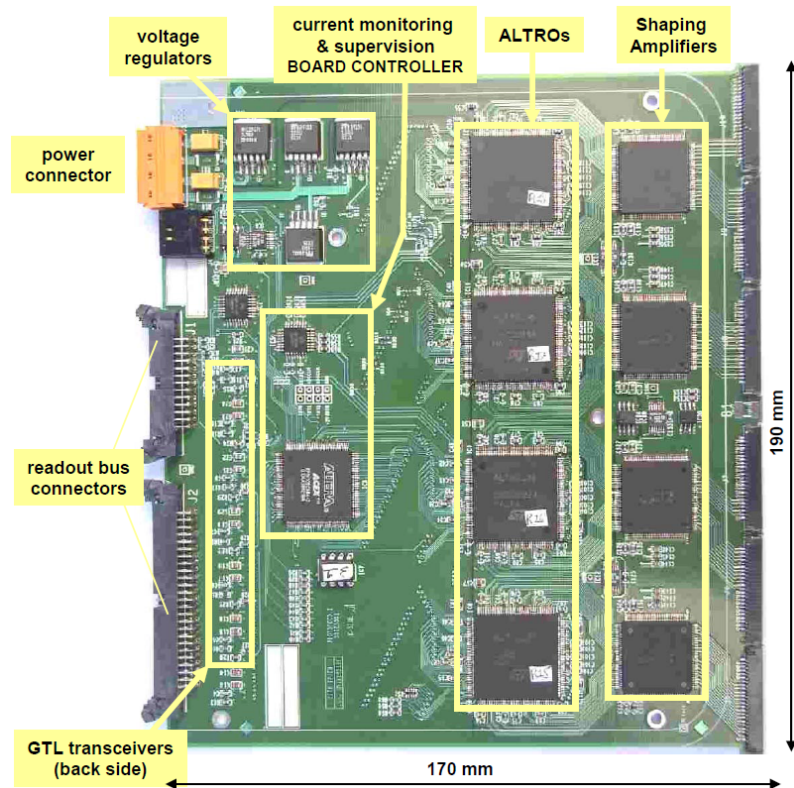


Figure 2.5: Top side of the Front End Card [13]

2.2.2 Readout Control Unit RCU

One Readout Control Unit (RCU) is connected to one row of FECs (up to 25 pieces), through a backplane³, see figure 2.3. The RCU task is to control all of the Front End Electronic (FEE) all the way from the readout pads through the FECs, and out to a Data Acquisition (DAQ) System. The RCU consist of three separated boards which are the Motherboard board, and the Control System board (DCS) board and a Source Interface Unit (SIU) board, which are attached to the Motherboard. Most of the RCU functions is controlled by the main FPGA, which is a Xilinx Virtex-II Pro FPGA. This FPGA is controlling the hole readout process of the TPC detector. It is also responsible of moving data from the FECs to the Source Interface Unit (SIU) board, where data is transmitted via a optical link to the Data Acquisition system, where data is stored and are accessible for the engineers.

The Xilinx Virtex-II Pro is a SRAM based FPGA. SRAM cells is especially vulnerable for Single Event Upset (SEU), see section 3.4.1. Therefore a flash based FPGA, Actel ProASIC is used to monitor the SRAM memory and reprogram/reconfigure if an error occurs.

The DCS board is basically a embedded computer running Linux. This board is connected through a Ethernet link to a computer on the outside of the ALICE detector. Through this Ethernet link we are able to upgrade and reprogram the FPGAs of the RCU. So even though the hardware is inaccessible after it has been mounted in the TPC, the SIU board gives us some kind of flexibility. In addition, it has an optical interface receiving the clock and trigger information from the Timing, Trigger and Control, also called TTC.

2.2.3 RCU2

Why upgrade RCU

LHC is currently shut down for maintenance and preparation for even higher energies. This period, called Long Shutdown 1 (LS1), lasts until end of 2014. The present TPC readout electronics will be a limiting factor with the foreseen readout rate for the next run period, called Run2. The bus between RCU and FECs are not able to read all data for high occupancy events, like Pb-Pb collisions. In addition stability issues related to SEU on the SRAM based FPGA have been observed with the present setup. 9% of the run time had to be stopped because of errors occurred in the TPC readout electronics.

³A backplane is a PCB board, that connects all of the Front End Cards to the Readout Control Unit. This is used instead of cables to get a more stability, and to keep things in place.

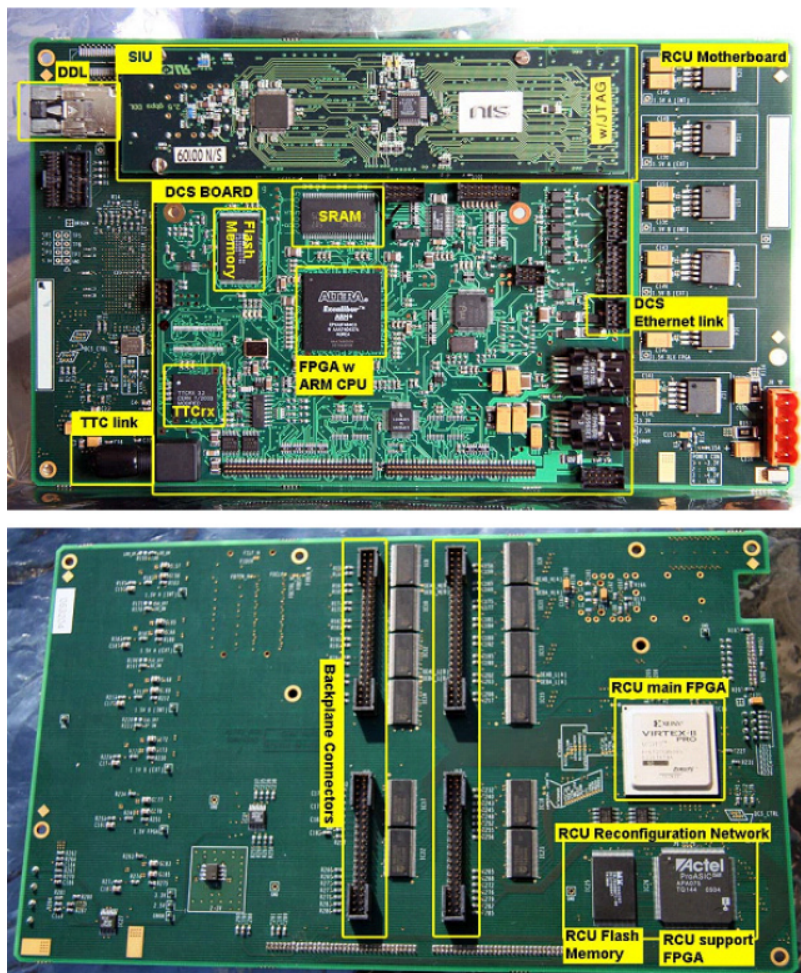


Figure 2.6: The Readout Control Unit top side and bottom side [13]

The new Readout Control Unit, the RCU2

The main motivation for the RCU2 was to develop a solution that gives the needed performance improvement, and at the same time was feasible within the limited time-frame. Therefore some of the old infrastructure has to be reused, like cables for Ethernet, Trigger and power and the cooling envelops. Since the infrastructure is basically the same, the size and placement of connector on the new RCU is the same as for the old one.

The main difference between the RCU2 and RCU1 is that the main FPGA, the Xilinx Virtex-II Pro, has been replaced by a Microsemi SmartFusion2 (SF2) System On a Chip (SoC) FPGA M2S050-FG896. This is a flash-based FPGA which has SEU immune configuration memory, as well as several other radiation tolerance measures implemented. It also comes with a Microcontroller Subsystem which is based on a hardcore ARM Cortex-M3 microcontroller. A Linux system is built on this Microcontroller Subsystem, which result in that we didn't need the Control System board (DCS) board anymore. The ProASIC was also not need as a reconfiguration FPGA anymore, but will still be used as a radiation monitor, this part of the RCU2 is now called RadMon, and consist of a ProASIC and SRAM chips. Another issue encountered in the design was that a chip called TTCrx chip that was used for handling the clock and trigger signal on RCU1 was out of stuck and obsolete. This will be replaced by a optical receiver and a limiting amplifier which has been tested in this thesis, see section 4.1.7.

One of the limits with the old setup was that the bus between RCU and FECs was to slow. This was fixed by dividing the readout into 4 sections instead of 2, which effectively doubled the readout speed. Therefore all of the backplanes had to be replaced with new ones.

3 Radiation and Radiation effect on Semiconductor devices

Radiation and radiation effects are a known challenge when designing electronics which are going to be used at CERN. There is therefore of highest importance to know about these effect, how they effect the electronics, how much damage they can cause and how we can protect and prevent the radiation effect to do damage.

Everything in this chapter is based on these references [15], [11], [10], [3] and [2] if not otherwise stated.

3.1 Interaction of Radiation With Matter

Radiation is defined as a process which energy in the form of energetic particles or electromagnetic waves is transmitted through a medium or space. Radiation is normally divided into two categories, that is

- Charged radiation
- Neutral radiation

Charged radiation consist of charged particles like protons(p), alpha(α) and beta(β) particles and heavier ions. Neutral radiation consist of neutrally charge particles like neutrons(n) and photons from gamma(γ) and X-rays. Particles who interact with a material will deposit some or all of its energy in the interaction, and can either interact with atoms, electrons, nucleus or the particles inside a nuclei. How much energy is deposited and which of these a particle will interact with is depended on the energy, mass, the charge of the particle and what material it interacts with. One of the main difference between charged particle and neutral particle is that charged particles will be effected by the Coulomb force, that is the attraction or repulsion of particles or objects because of their electric charge. In the next sections we will look more closely on how a charged particle and neutral particle interact with matters.

3.2 Charge particle and their Interaction with Matters

When a charged particle with high speed is passing through a material it will experience multiple elastic and inelastic collisions with the atoms in the material, resulting in slowing down or stopping the particle. When a particle collide with a atom there are several process that can contribute to the loss of energy. They are:

- Inelastic scattering towards atomic electrons
 - Excitation and ionization
- Elastic scattering towards atomic electrons
 - Ramsauer Effect
- Inelastic scattering towards Nuclei
 - Nuclear reaction
- Elastic scattering towards Nuclei
 - Rutherford/Nuclear scattering
- Other processes
 - Bremsstrahlung and Cherenkov radiation

Which of these that contributes to most of the loss of energy is depended on the initial energy, velocity, mass and charge of the particle as well as the properties of the material it collides with. For example, for heavy charge particles(protons or heavier ions), inelastic collisions with the atomic electrons in a material will contribute to most to the energy loss of the particle. A common expression for these processes is called "stopping power".

3.2.1 Stopping Power

If we have a particle with a given energy passing into to a material, where dE is the mean energy that the particle losses by traveling through a path segment, dx , of the material. Then $-\frac{dE}{dx}$ is the stopping power or also called the "rate" of energy loss for the particle. The stopping power depends on the type and energy of the radiation and on the properties of the material it passes.

The classical expression that describe the stopping power is the *Bethe Bloch formula*, and is written as you can see in equation 1.

$$S = -\frac{dE}{dx} = \frac{n_A Z_A Z^2 e^4}{4\pi\epsilon_0 m_e V^2} \left[\ln\left(\frac{2m_e v^2}{\bar{I}}\right) - \ln\left(1 - \frac{v^2}{c^2}\right) - \frac{v^2}{c^2} \right] \quad (1)$$

| | |
|--------------|---|
| n_A | Number of atoms per unit volume |
| Z_A | Average atomic number of the material |
| Z | Atomic number of particle |
| e | Electron charge |
| c | Speed of light |
| ϵ_0 | Vacuum Permittivity |
| m_e | Electron rest mass |
| v | Particle velocity |
| \bar{I} | Effective material ionization potential |

3.2.2 Specific Stopping Power

Another way of looking at stopping power, is by looking at energy loss as function of mass per area 2. Here $\xi = \rho x$ and ρ is the density of the material. The extension for specific stopping power is normally given as $[\frac{\text{MeVcm}^2}{\text{g}}]$

$$S = -\frac{dE}{d\xi} = -\frac{1}{\rho} \frac{dE}{dx} = -\frac{n_A Z_A Z^2 e^4}{4\pi \epsilon_0^2 m_e v^2} \left[\ln\left(\frac{2m_e v^2}{\bar{I}}\right) - \ln\left(1 - \frac{v^2}{c^2}\right) - \frac{v^2}{c^2} \right] \quad (2)$$

From this formula we see that if considering different particles with the same velocity, then the only factor that changes are Z^2 . Therefore heavier particles will experience larger energy loss in a material than lighter ones. In figure 3.1 we can see specific energy loss for different particles in air. We can see that the value of $\frac{dE}{dx}$ for different types of particles approaches a near-constant broad minimum value at energies above several hundred MeV, where their velocity approaches the velocity of light.

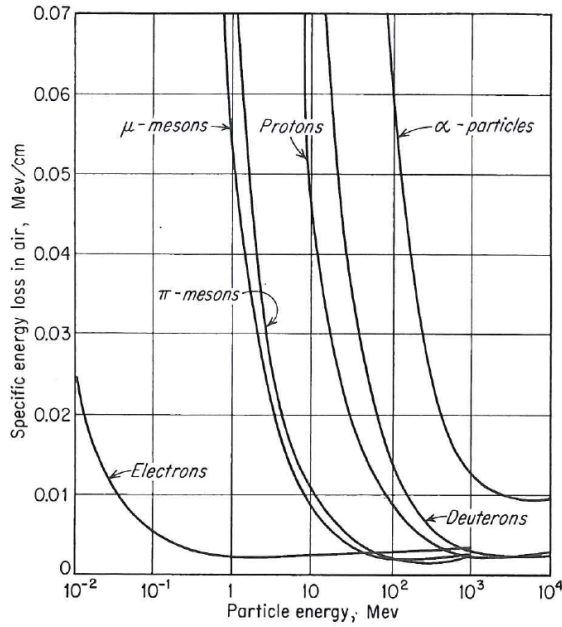


Figure 3.1: Variation of the specific energy loss in air versus energy of the charge particles shown

At low particles energies, where charge exchange between the particles and absorber becomes important, the Bethe Bloch formula begins to fail. That is because the positively charged particles will then tend to pick up electrons from the absorber, which effectively reduce its charge and consequently linear energy loss, and will at the end become a neutral atom.

3.2.3 Linear Energy Transfer LET

Linear Energy Transfer (LET) is closely related to stopping power of a particle, but instead of focusing on energy loss of the particle, LET focuses on the energy that is deposited in a local volume. For low energies, LET is often said to be equal stopping power, even though the particle energy that turn into photons may escape the local area. For higher energies, small particles like ionized electrons can escape the local volume. The local volume is defined by yourself, and can be everything from part of a molecule to a hole organ. One alternate definition of LET can be seen in equation 3

$$L_{\Delta} = \left(-\frac{dE}{\xi x} \right)_{\Delta} \quad (3)$$

where Δ is the upper energy limit for the secondary electrons included in the calculations. If Δ is set to ∞ , all secondary electrons are included in the calculations,

making LET the same as stopping power.

3.3 Neutral particle and their Interaction with Matter

3.3.1 Neutrons

Neutrons are subatomic structure that are present in most atomic nuclei. Neutrons carry no charge and can therefore not interact with matter by means of the coulomb force, which dominates the energy loss mechanisms for charged particles. Neutrons can also penetrate several centimeters into matters without any type of interactions, making neutrons hard to detect. When neutrons undergo a interaction, it is with the nucleus of the absorbing material. This can result in total disappearance of the neutron resulting in one or more secondary radiations, or change of the direction of the neutron. The secondary process of neutrons can largely ionizing.

3.3.2 Photons

Photons may appear from gamma rays or X-rays. Photons has as neutrons no charge, and are therefore not effected by the coulomb force, additionally photons has no rest mass and travel in constant speed of light. The energy of a photon is given in the formula $E = hf$ where f is the frequency of the particle and h is the Planck's constant. There are three main process where a photon may react with matters, they are:

- Photo electric effects
- Compton scattering
- Pair production

3.4 Radiation Effects on Semiconductor Devices

Semiconductor devices planned to used in a radiation environment are likely to be effected by the radiation in some way. If not taking properly into account, the radiation effects may damage or even destroy the electronics. Therefore there is of highest importance to know about how irradiation can effect the semiconductor devices. We normally divide radiation effects in two groups that is *Singel Events effects* and *Accumulative Effects*.

3.4.1 Single Events Effects SEE

Single Event Effects are due to the energy deposited by one single particle in the electronic device. Therefore, they can happen in an moment, and their probability is expressed in terms of cross-section [7]. This effects has been an increasing problem as the manufacture process are getting smaller and smaller, making circuits more weak for radiation. In the next sections we will look into three SEEs, that is Single Event Latchup (SEL), Single Event Transient (SET) and Single Event Upset (SEU).

Single Event Latchup SEL

A Single Event Latchup (SEL) is phenomena where a low resistance path between power and ground is formed, normally resulting in burned traces, which means reduced performance or destruction of the chip. Therefore it is of highest importance to know about this effect, to know how to counter or to protect from latches in design phase. In a Complementary Metal Oxide Semiconductor (CMOS) process a SEL can occur when a ionized particle penetrate the silicon in a transistor causing a charge to turn ON the parasitic bipolar transistors formed by the substrate, well, and the diffusion. This will result in a low resistance path between power and ground, and a high current will flow. If a SEL has occurred, power to the chip needs to be turned off immediately, before the high current flowing from power to ground will burn interconnections and permanently set the chip out of function.

How a latchup may occur can be understood by looking at a CMOS inverter, see figure 3.2. From figure 3.2(a) you can see a resistor formed in the well and substrate, and a parasitic bipolar npn-transistor and pnp-transistor formed inside the inverter. An equivalent circuit can be seen in figure 3.2(b). Originally both of the bipolar transistors are turned off, and no current flows through the transistors. A latchup can be triggered if a ionizing particle flows into the substrate creating a transient current that can set V_{sub} high, causing npn-transistor to turn ON. If the npn-transistor turns ON, then current will flow trough R_{well} causing V_{well} to go low, and setting pnp-transistor ON. When the pnp-transistor turns ON current will flow through R_{sub} , causing V_{sub} to rise, and we have created a positive feedback, causing high current to flow from power to ground.

Single Event Transient SET

Single Event Transient (SET) is a transient pulse of current in a logical path of a circuit. A SET is caused by an ionizing particle leaving a transient current close or on a sensitive circuit node. This current can cause a change of value on that node for a short time, and if this value is clocked in on a register, we will have an unwanted change of value and that is called a SEU. If this value is not clocked out or saved in some way, the current peak will just flat out, and nothing will happen. A way to detect SET could be to make a shift register made up of a known number

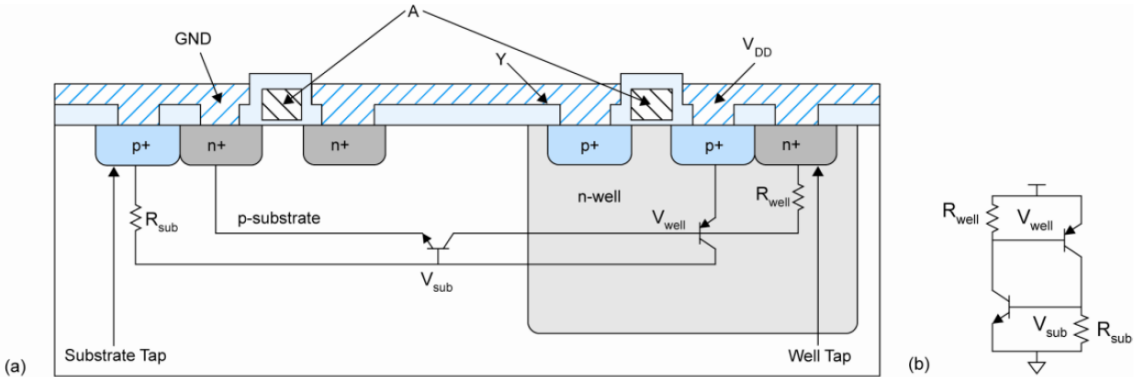


Figure 3.2: (a) A CMOS inverter with parasitic bipolar transistors (b) A model of the parasitic circuit

of register and a known input data. By checking the output and compare with the known value, you can detect if a SET has occurred.

Single Event Upset SEU

Single Event Upset (SEU) is change of state in a logical element, caused by radiation. This phenomena can often be seen in memory cells or registers, where data is stored. A SEU is a "Soft error", which means that it is a non-destructive type of error. By resetting or overwriting after an SEU has occurred, the error will disappear.

For better understanding of SEU we can look at a six transistor SRAM cell, see figure 3.3. If we say that $Q = '0'$ and $Q.b = '1'$, so there is a value '0' written to the cell. Then a high energetic neutron strikes into the drain of transistor D_2 and hits a silicon atom. This cause shattering of the atom into charged fragments (ions) that travels through the substrate. These ions leaves a trail of electron-hole pairs, see figure 3.4(a). When the resultant ionization track traverses or comes close to the depletion region, carriers (electrons) are rapidly collected by the electric field creating a large current transient (SET) at that node, causing voltage drop at the node $Q.b$. If this voltage drop is high enough, transistor P1 will be opened up, and transistor D1 will be closed, causing Q to go towards '1' which again causing P2 to close and D2 to open up causes $Q.b$ to be discharged through D2, and set to '0'. Then the SRAM cell has changed value from '0' to '1', and we have a SEU.

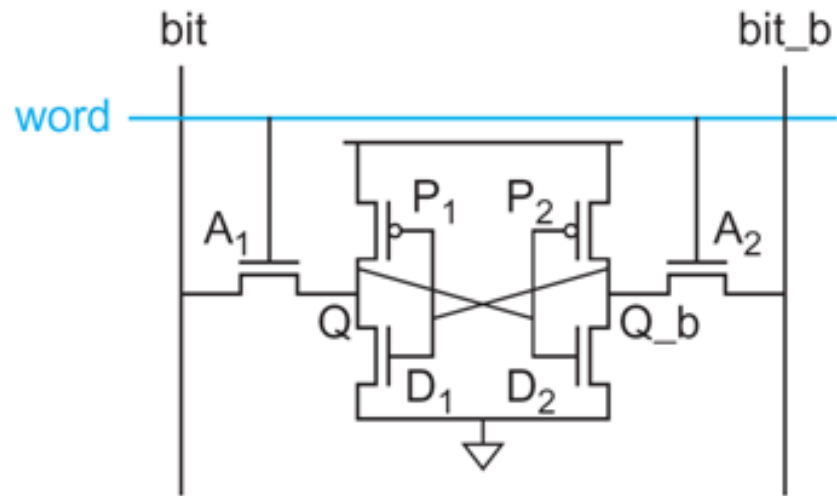


Figure 3.3: Six transistor SRAM Cell

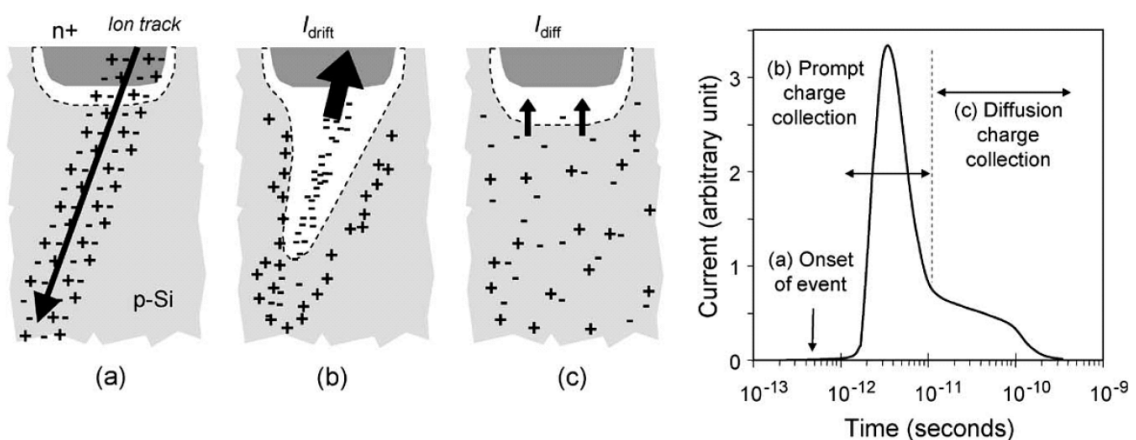


Figure 3.4: (a) Electron hole pairs generated (b) Carrier are drawn towards the depletion region causing a current jump (c) Additional charge is collected on a more long time scale (hundreds of nanoseconds) [3]

3.4.2 Accumulative Effects

Accumulative effects are energy deposition caused by radiation for the whole lifespan of a circuit [7] and [16]. Accumulative effects are measured by the functionality of a device, and power consumption. Some circuits are weak for accumulative effects, and will stop working only after a small dose of radiation, but others device may not even have any effect after a severe dose of radiation. When a chip stops working, we say that it has reached its tolerance level. When we talk about accumulative effects we normally divide into two groups, that is displacement damage, which is a non-ionizing effect, and TID which is a ionizing effect.

Total Ionization Dose TID

Total Ionizing Dose (TID) is measurement of the dose, that is the energy, deposited in a circuit by radiation in the form of ionization energy. The unit used are Gray (Gy) or rad. The relation between those two can be seen in equation 4.

$$1\text{Gy} = 100\text{rad} \quad (4)$$

The heart of TID effects is the energy deposition in the silicon dioxide. When ionizing particles penetrates into a transistor, electron-hole pairs will be created. Most of the pairs will recombine shortly after they are generated, but some do not completely recombine because of the electric field. Electrons, with high mobility, can easily leave the oxide, but holes are lower mobility and can be trapped in their point of generation in the oxide. The trapped holes cause a negative threshold voltage shift in the MOS transistor, and if enough holes are trapped, it can result in a transistor which is permanently ON. This phenomena can be seen in figure 3.5.

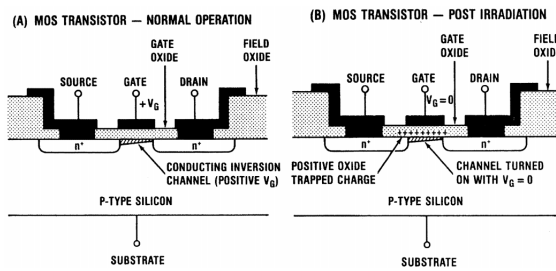


Figure 3.5: Layout of a MOS transistor. (A) shows normal operation and (B) shows the transistor after irradiation.

Displacement Damage

Displacement Damage is a non-ionizing effect mostly induced by low energetic particles colliding with and breaking atoms out of the initial lattice structure of a material. This can affect the functionality of the device. CMOS circuits are

normally considered immune to this effect. Displacement damage is not measured in any unit, but it is expressed in terms of the particle fluence, in particles/cm².

3.4.3 The TPC radiation environment

The radiation in the LHC is dominated by high energetic neutrons and protons, mostly neutrons with a estimated fluence of $(0,6 - 1,1) \times 10^{11}$ *neutrons/cm²*. Therefore it would be preferable to test our electronics with a neutron beam, but since there are few labs who can produce a neutron beam compared to proton beam most of the electronics is only tested at OCL with a proton beam. There has been done experiment that compares SEU induced by neutrons and protons [8], and the result shows that it is possible to use a proton beam instead of proton beam with small deviations. By comparing a Proton beam with a neutron beam of 21MeV we see that we get 10-25% less SEU cross section for a proton beam compared to a neutron beam. If we increase the energy to 88MeV then we get close to none deviations.

The dose that we could expect for a 10 year period in the ALICE detector is estimated to be approximately 0.6 kRad from Pb-Pb collisions that will be run 1 month a year and a little higher for p-p collisions that will be run 10 months a year [17] and [13]. Therefore we could expect a dose of 1-2 kRad during the time it will be used at CERN.

4 The Test Chips and Preparations for Testing

Testing Integrated Circuits (ICs) is a thing that has been done before when it comes to the design of electronics that are going to be installed in the LHC at CERN. Much of the work presented in this thesis is based on experience from previous thesis [14] [13] [12] [18].

4.1 The Integrated Circuits Which Where Tested

The IC that was tested through this thesis are: TPS51200, MIC69302WU, SN74AVCB164245, SN74AVC2T245, QS3VH257, SY89831, ADN2814, MAX3748, INA210, TLV3011 and SF2 M2S050-FG896. What each of these are, and how these was tested will be discussed in the following sections.

For each of the different IC, except for SF2, a Printed Circuit Board (PCB) was made with only the necessary electronics to make it work and to be able to test the functionality of the IC. Connectors (1-2) was placed on the PCBs and connected to Data Acquisition (DAQ) boards from National Instruments. These gave us the possibility to control the inputs of each IC and monitor the outputs. A small resistor was placed in serial with the power input, so we would be able to measure the voltage over this resistor to get current.

We wanted to have two PCB for each of the IC that was going to be tested to have more test data on each IC, and to be sure that the error we would see wasn't just a coincidence. There may be some difference between two boards made for the same chip, that is because the first board made may have some modification on the PCB, to make it work. When the second board was made, error or mis functions was fixed at PCB level. So that modification wasn't needed. The second version was tested first, in case we didn't have time to test both of the versions. Later in this thesis the second board that was made are marked with ₁ and the first board was marked with ₂. Two of the ICs (ADN2814 and MAX3748) was only made one version of, since we didn't have any spare IC at the time to make a new PCB. All of the test PCBs had a mark on the back indicating the center of the IC, this was used to pinpoint the center during the tests.

To supply and measure everything on the test boards, Data Acquisition (DAQ) devices from National Instruments were used. The DAQ devices we used are called USB-6009, USB-6008 and USB-6501. USB-6009 was used as the main one, and the other were used when needed more digital or analog inputs or outputs. USB-6009 has 8 single-ended analog input (AI) channels, 2 analog output (AO) channels and 12 digital input/output (DIO) channels, and also a 2.5 V and 5.0 V signal. The analog outputs has a limit of 5 mA, but some of the ICs that was tested required

more than that. For these cases the 5 V signal was used, that can deliver current up to 200 mA. More information on the DAQs can be seen in the reference [5].

4.1.1 TPS51200

This is a adjustable power regulator from Texas Instruments. It is special designed for DDR RAMs, it can be used for DDR, DDR2, DDR3 and DDR4 applications.

In figure 4.1 you can see a schematic layout of the PCB board for the TPS51200. The PCB was designed after a recommended setup for DDR3 application from the datasheet [9]. Input voltage was set to 3.3 V. Voltage over resistor R1 (See figure 4.1) was measured and used to calculate current consumption. Output voltage was also monitored.

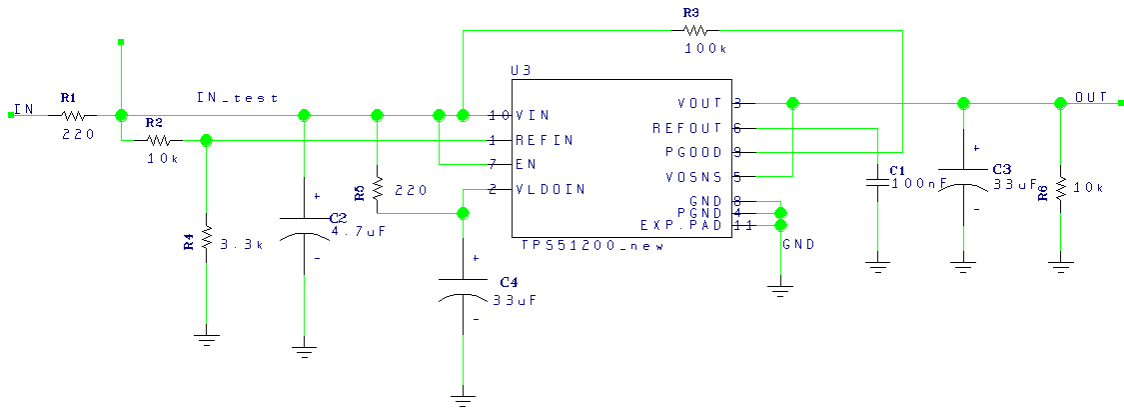


Figure 4.1: Schematic for the TPS51200 test board

4.1.2 MIC69302WU

This is a ultra low dropout¹ adjustable power regulator from Micrel Incorporation. It is in a family of high current, low voltage regulators, and can deliver a current of up to 3 A.

This is a adjustable regulator. That means that by changing R1 and R2(see figure 4.2) you can adjust the output voltage, see equation 5. For the two test boards we had a input voltage of 3.3 V. Voltage over resistor R?(See figure 4.2) was measured and used to calculate current consumption. Output voltage was also monitored. We used 10k Ω for both R1 and R2 which gave us 1 V on the output.

¹Low dropout means that voltage on the output can be close up to the input. For MIC69302WU low dropout means that $V_{IN} - V_{OUT}$ can be as low as 500 mV

A third PCB was made with this IC. This was used to supply 3.3V to the PCB that requires more than 5 mA which is the maximum the analog outputs the DAQ from National Instruments can deliver. This was designed with resistor values of $R_2 = 20 \Omega$, $R_1 = 5.6k \Omega$ and $R_2 = 1k \Omega$, which gives us 3.3 V output. This PCB was used to supply SY89831U, ADN2814 and MAX3748

$$V_{out} = 0.5 \times \left(\frac{R_1}{R_2} + 1 \right) \quad (5)$$

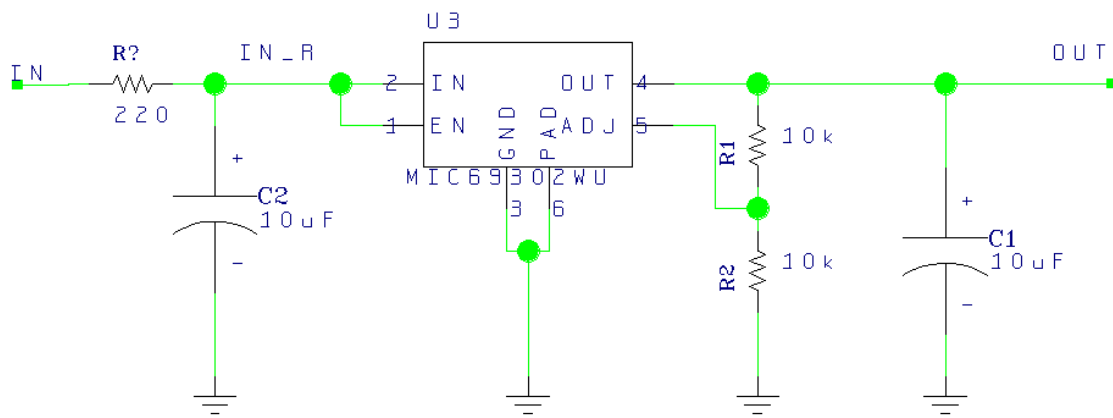


Figure 4.2: Schematic for the MIC69302WU test board

4.1.3 SN74AVCB164245

This is a 16-bit noninverting bus transceiver, with configurable voltage. Used for level shifting for digital signals. An application example could be to convert a 16-bit digital signal that has a high value of 1.5 V to a 16-bit signal with a high value of 3.3 V. The input and output high value can be set to anything between 1.4 and 3.6 V, the low value is set to 0 V.

For the test board the supply voltages(VCCA and VCCB, see figure 4.3) was both set to 3.3 V to make it more simple to test. Voltage over resistor R1 (See figure 4.3) was measured and used to calculate current consumption. To make sure that the circuit didn't draw current through the inputs on the chip we used a pMOS transistor that was connected as seen in figure 4.3. This made the current for the inputs come from the supply pin, and not from the digital signal IN. The outputs was measured digitally.

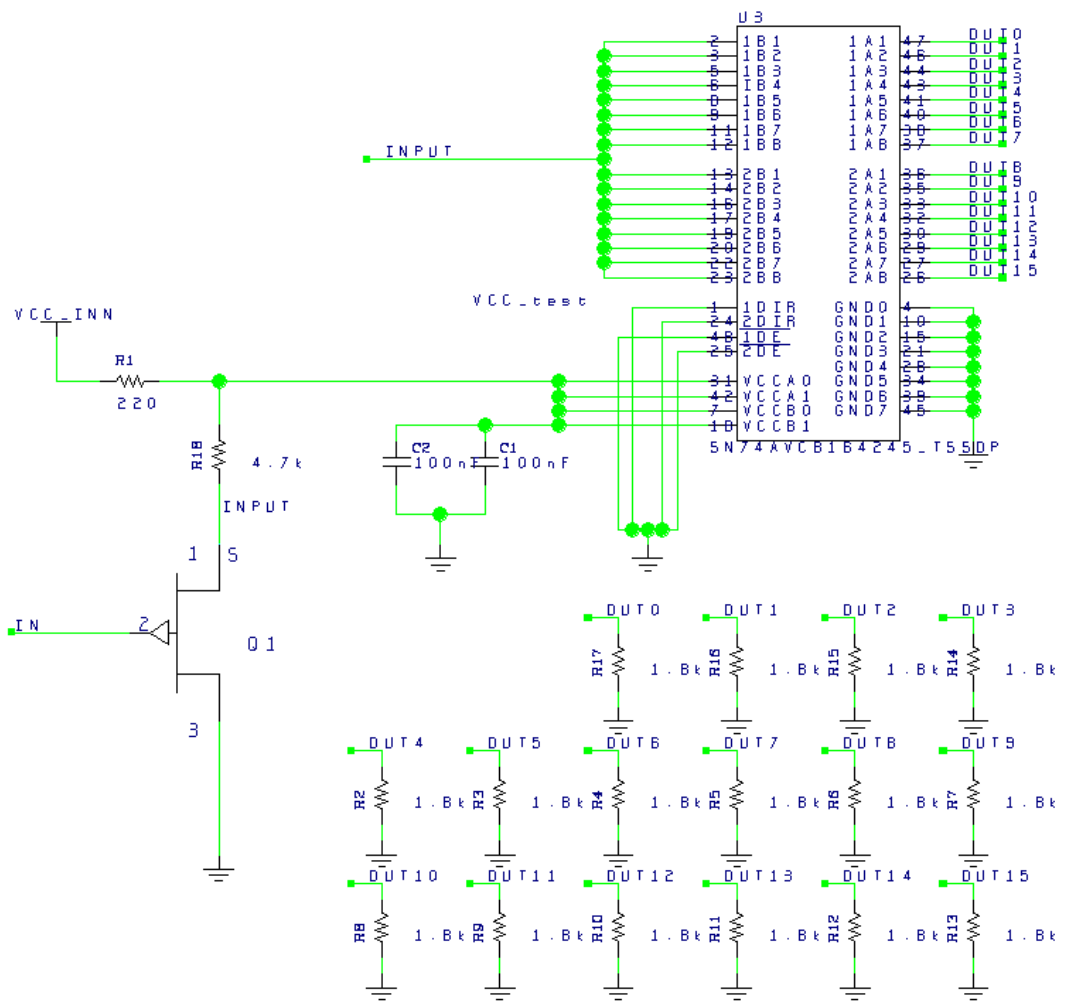


Figure 4.3: Schematic for the SN74AVCB164245 test board

4.1.4 SN74AVC2T245

This is a dual-bit noninverting bus transceiver, with configurable voltage. It has the same function as SN74AVCB164245, but this only has two inputs.

As for SN74AVCB164245 a 3.3 V supply was used for both VCCA and VCCB, see figure 4.4. Voltage over resistor R1(See figure 4.4) was measured and used to calculate current consumption. The output signals was monitored digitally.

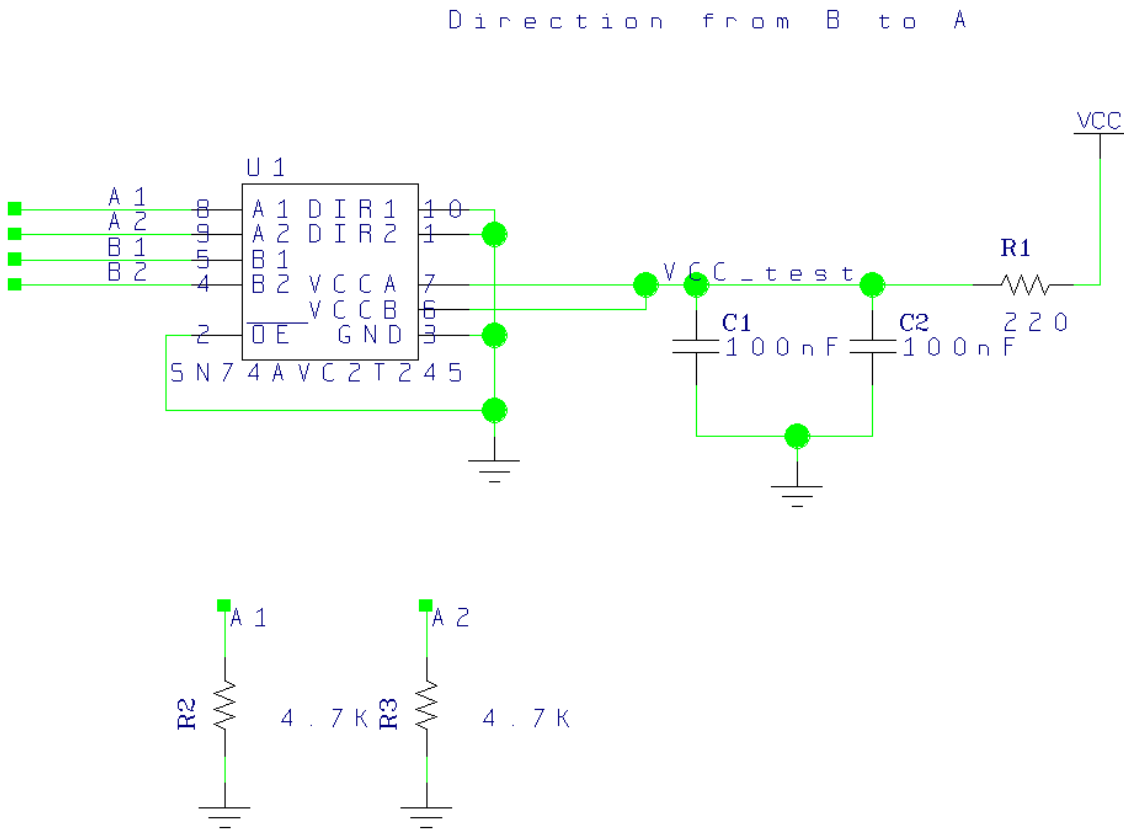


Figure 4.4: Schematic for the SN74AVC2T245 test board

4.1.5 QS3VH257

This IC consist of four 2 to 1 multiplexer/demultiplexer. It has high bandwidth, up to 500 Mhz, low ON resistance and high OFF resistance.

Supply voltage was set to 3.3 V. Voltage over resistor R1(See figure 4.4) was measured and used to calculate current consumption. For the Select input a analog output signal was used. The input signals was set digitally, and the outputs was measured digitally.

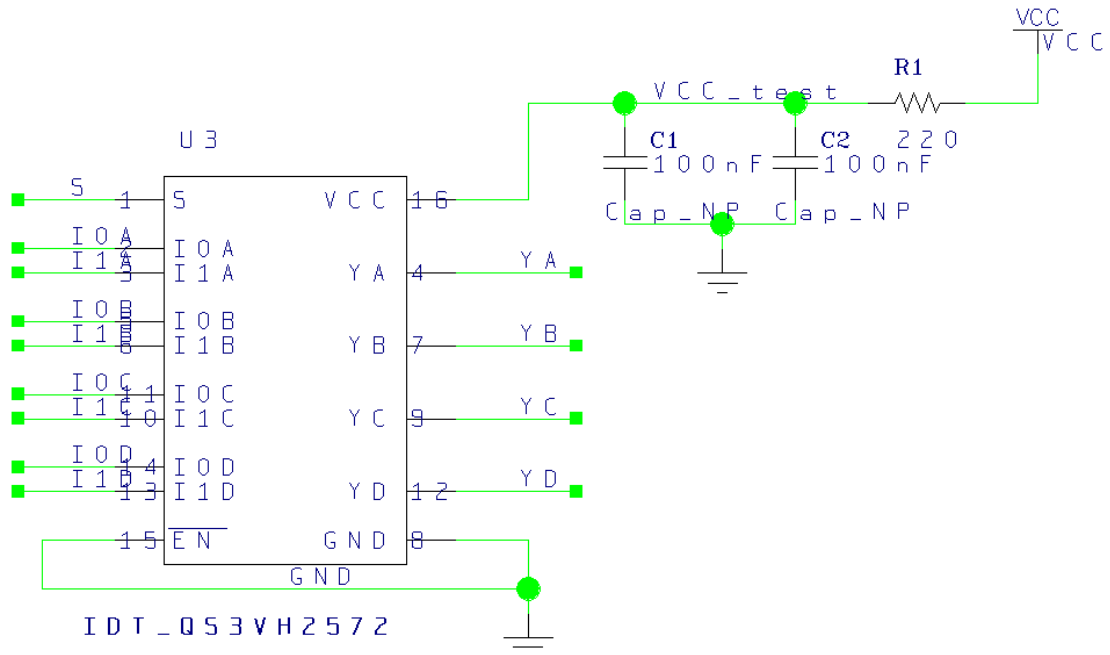


Figure 4.5: Schematic for the QS3VH257 test board

4.1.6 SY89831U

This is a high speed, 2GHz differential Low Voltage Positive Emitter Coupled Logic (LVPECL) 1 to 4 fanout buffer optimized for ultra-low skew applications.

The input signal to this IC is differential. The DAQ device we were using doesn't have a differential output signal, so here we had to use a little trick to make it work. We used two single-ended output signal that was set to the opposite of the other, and every 100 ms the values switch, so that when IN+ was 3.3 V IN- was 0 V, and when IN+ was 0 V IN- was 3.3 V. The outputs was measured by the analog inputs of DAQ USB-6501.

This IC requires a large current typically around 60 mA, and we could therefore not use the analog outputs. So we had to use the modified version of the MIC69302WU PCB, that will supply us with a 3.3 V signal up to a current of 200 mA.

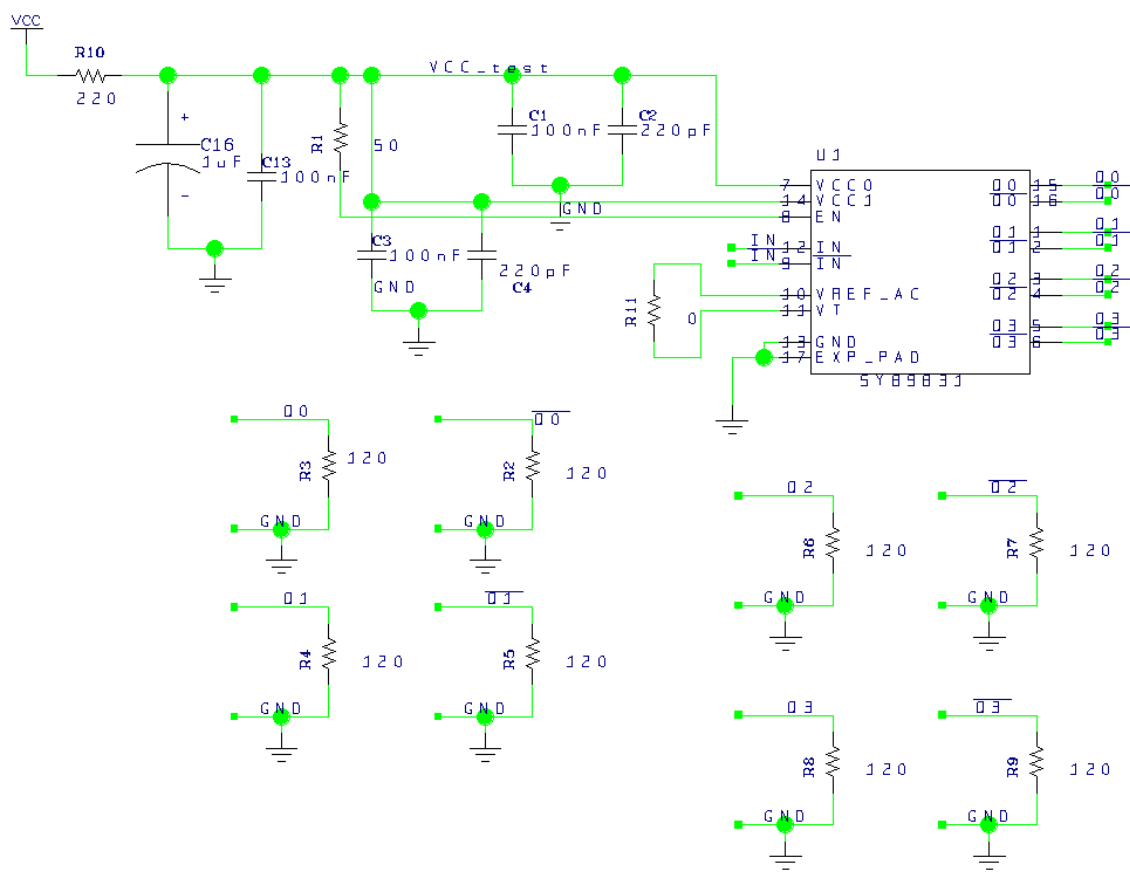


Figure 4.6: Schematic for the SY89831U test board

4.1.7 ADN2814 and MAX3748

These two boards are used for the same purpose, and the one of them that performs best will be chosen to be used on the RCU2. ADN2814 is a clock and data recovery IC with integrated limiting amplifier. Works in rate of 10 Mb/s to 675 Mb/s. Gives out a Low-Voltage Differential Signaling (LVDS) clock and data signal. MAX3748 is a limiting amplifier. Works in rate of 155 Mb/s to 4.25 Gb/s. Gives out a Current-Mode Logic (CML) data output signal.

These ICs are going to be used to make a stable LVDS or CML signal from an optical transceiver. The signal from the optical transceiver is a Manchester coded signal consisting of data and clock. There are a few differences between the two ICs. MAX3748 comes in a smaller package and uses less power and works in higher rates, but it doesn't have a clock return function as as ADN2814 has. Both works for our specific use, therefore we will see from the test results which one will be used.

The two limiting amplifiers (ADN2814 and MAX3748) required a more advance inputs, and therefore a SmartFusion2 (SF2) starter kit are going to be used in addition to labVIEW. The SF2 board was used to code a clock and data signal into a differential Manchester signal and to decode the differential Manchester signal back to clock and data after it has gone through the IC. The SF2 was also used to compare the original signal with the signal coming out from the IC. A picture of the Smart Design can be seen in figure 4.16. This consist of IP-cells from Microsemi and some VHDL code that has been made.

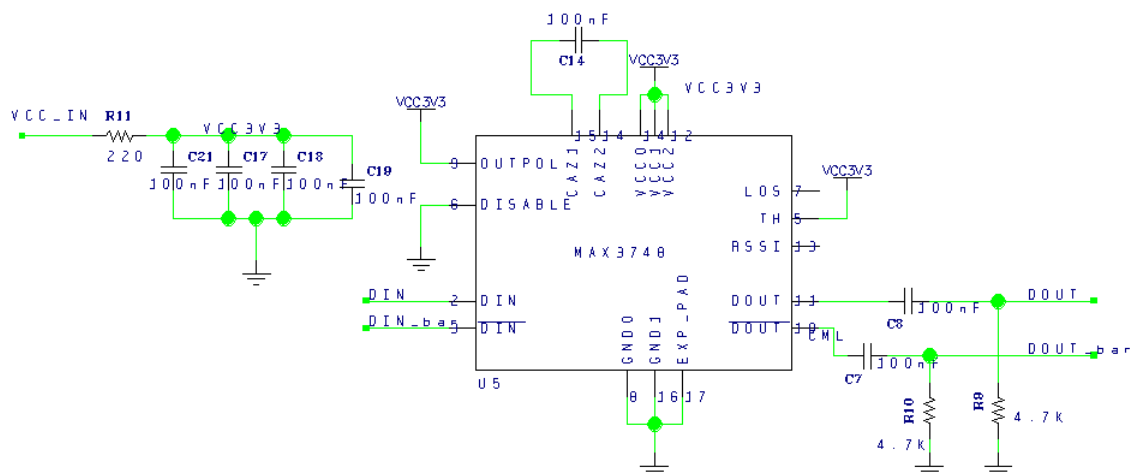


Figure 4.7: Schematic for the MAX3748 test board

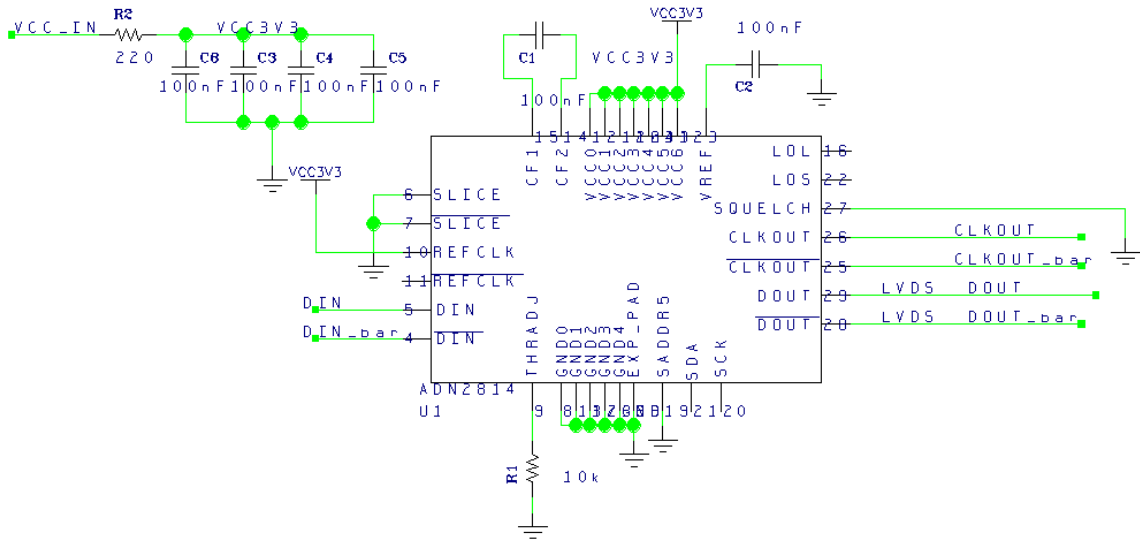


Figure 4.8: Schematic for the ADN2814 test board

4.1.8 INA210

INA210 is a so called Current-Shunt Monitor, that is a IC that is used to amplify small current signal into higher voltage signal. This is done by sending the signal that you want to measure current of, over a small resistor, typical smaller than 1 Ohm. Then a voltage will be formed over this resistor and will be amplified through the IC. This IC comes in a family of 5 with different amplifications, the one we are using has an amplification of 200 V/V.

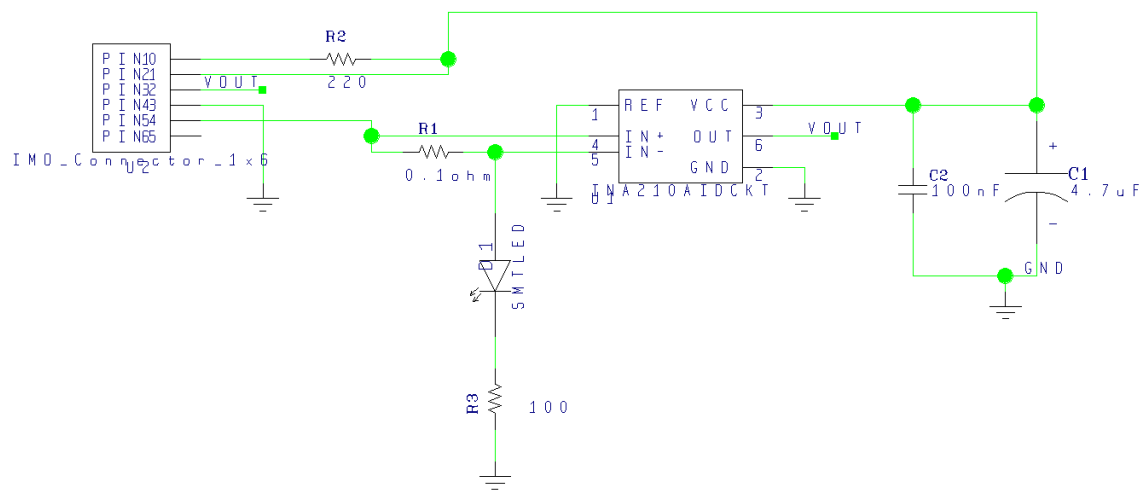


Figure 4.9: Schematic for the MAX3748 test board

4.1.9 TLV3011

This is a comparator with a built in voltage reference of 1.242 V. It supports low supply voltage from 1.8 V to 5.5 V, and has a open-drain output with fast response time. A 10 kOhm resistor is needed as pull-up on the output.

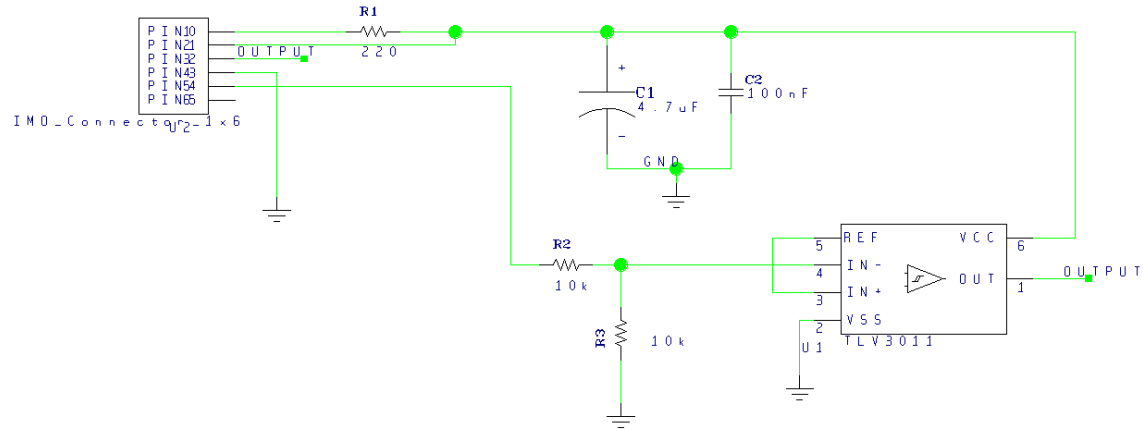


Figure 4.10: Schematic for the MAX3748 test board

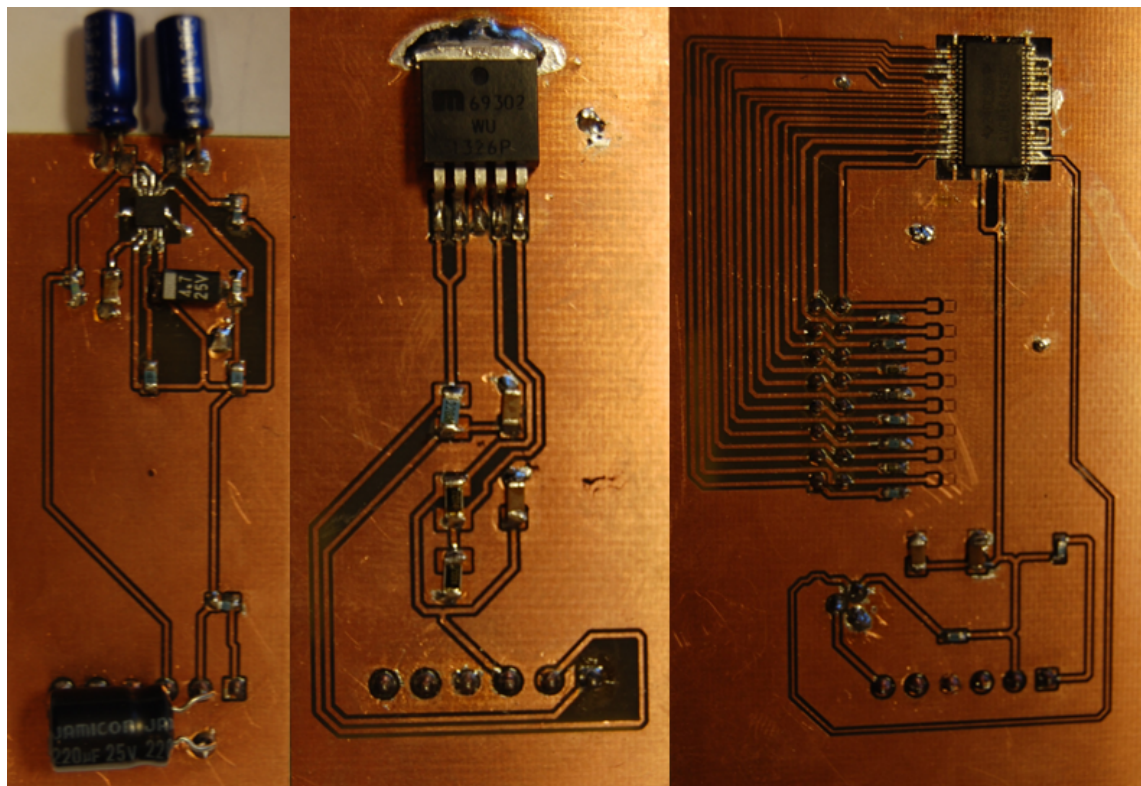


Figure 4.11: Picture of PCB boards, from left we have, TPS51200, MIC69302WU and SN74AVCB164245

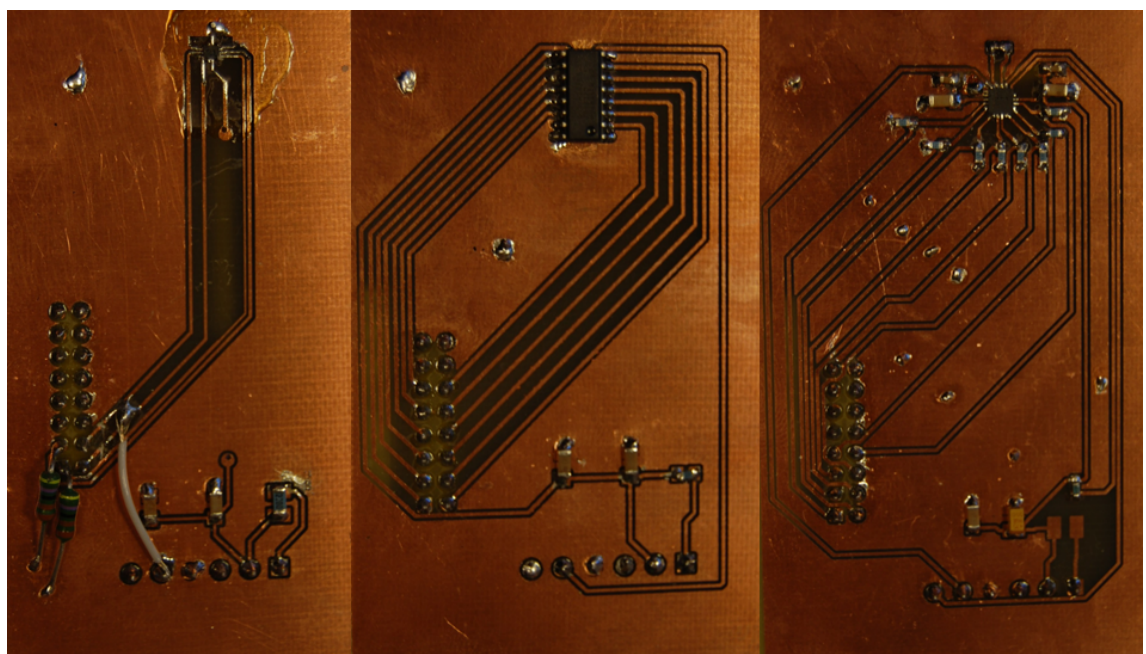


Figure 4.12: Picture of PCB boards, from left we have, SN74AVC2T245, QS3VH257 and SY89831U

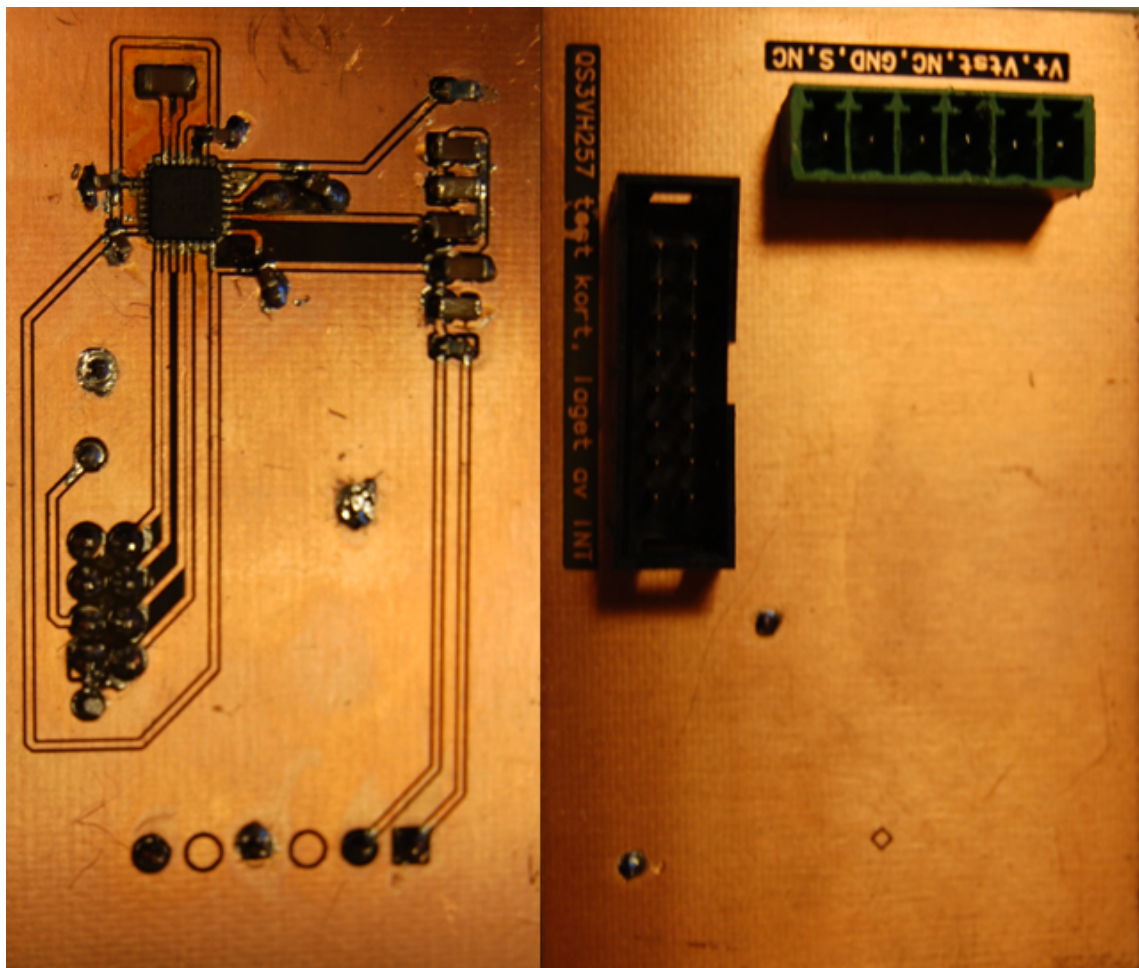


Figure 4.13: Picture of PCB boards, from left we have, ADN2814, MAX3748. plus an example of a back side QS3VH257, you can see the mark at the top indicating the center of the IC

4.1.10 SmartFusion2

SmartFusion2 (SF2) SoC FPGA integrate a flash-based FPGA², an ARM Cortex-M3 processor built in a Microcontroller SubSystem (MSS) and high-performance communication interfaces on a single chip. It is also said to have immune configuration memory, as well as several other radiation tolerance measures implemented. We are going to use the package M2S050-FG896, with a FPGA of 56 340 logic elements, 6 PLLs, 1314 kb RAM, 8 SERDES³ lanes, and 377 user I/O.

There are four things that we wanted to test on the SF2 chip. That is the internal SRAM blocks, the logical element, the PLLs and Single Event Latchup (SEL) for the hole IC. How these will will be discussed in the following sections

SRAM testing

SRAM cells are as discussed in section 3.4.1, sensitive for radiation. The SRAM memory aren't used for configuration register, as it was for the Xilinx FPGA on RCU1, and are therefore not as critical. But we still want to test how robust the SRAM cells are against radiation, so we can know how reliable these are if used. The SRAM blocks on the SF2 are divided up into 72 micro SRAM blocks with a size of 64 x 18 bits, and 69 Large SRAM block with a size of 1024 x 18 bits. Both micro SRAM blocks and large SRAM blocks are so called two port SRAM, which means that we can read and write at the same time.

The way the SRAM memory was tested is divided into 3 state in a state machine, this can be seen in block diagram in figure 4.14. The first state is a reset state, where all values are set to its nominal value. That means all counter is set to 0, write address is set to 0, read address 1, and write data is set to 1010...1010. Read address is always set be one higher then read address.

The next state is a initial state where all addresses are written to. Write data is switched opposite every address increment, so the written data is switched between 1010...1010 and 0101...0101 every other address. When the last bit is written to, the first bit is read.

The last state is a state where all of the addresses are written, read and compared through an endless loop. The written data is always opposite of the previous value written to that address. The state machine will stay in this state until a reset is pushed.

²Flash based FPGA means that configuration registers is saved in flash memory cells. Compared to SRAM-based FPGA, flash based FPGA is much more robust against radiation.

³Serializer/Deserializer (SERDES) convert data between serial data and parallel interfaces in both direction

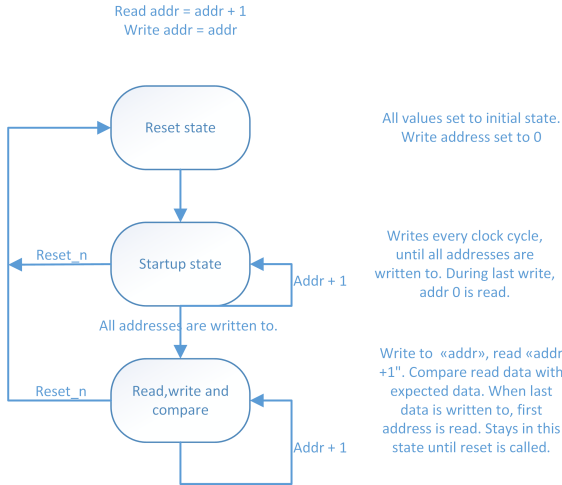


Figure 4.14: Flow chart for test procedure of SRAM

Test of the Logical element

A logical element consist of a 4 input Look-Up Table⁴ and a separate flip-flop which can be used independently from the Look-Up Table. That means that we have 56 340 flip-flops and 56 340 Look-Up Tables available for our design. When a logical element is exposed to radiation, a SET can occur all over the chip. If this happens in the logical element or in the interconnections between logical element, the transient current will normally just be there for a small amount of time, and then it will flat out, causing no error or bit flip in the chip. But if this transient current hits a sensitive node as the input to a flip-flop, or a other node that lead to changed value at the input node, and the input is then clocked out to the output, we would have unwanted bit change or a so called SEU.

The way we tested the logical element is based on [4], which has done a study on how to test FPGAs in a good manner. A good overview of the design can be seen in figure 4.15. The idea is to make a long serial chain of flip-flops, otherwise referred to as a shift-register, where a transient can be picked up. By adding a even number of inverters in between each flip-flop we increase the area where an transient can occur, without changing the logic. A known pattern is added to the input of the shift-register, this can be change depending on how advanced you want to be, but typical and easy pattern could be even other '1' and '0'. To be able to operate at high speed, we are using something called Windowed Shift Register (WSR), which takes out the last n-bit of the shift register, and sends it out in parallel, with a frequency n times lower then original frequency. To test check the output for errors, the WSR bits will be sent through the I/O-pins to another SF2 starter kit, hereafter referred to as the monitoring board, where data is checked by comparing with a known pattern. To be able to synchronize the two board, a reset signal and shift enable signal will be sent from the monitoring board to the test board, and a WSR enable signal will be sent from the test board to the monitoring board.

For our tests we made 4 shift-register chains, with 4 inverters in between each

flip-flop and where each of the shift-register had a 4-bit WSR output. The length of the shift-registers was set to 2000.

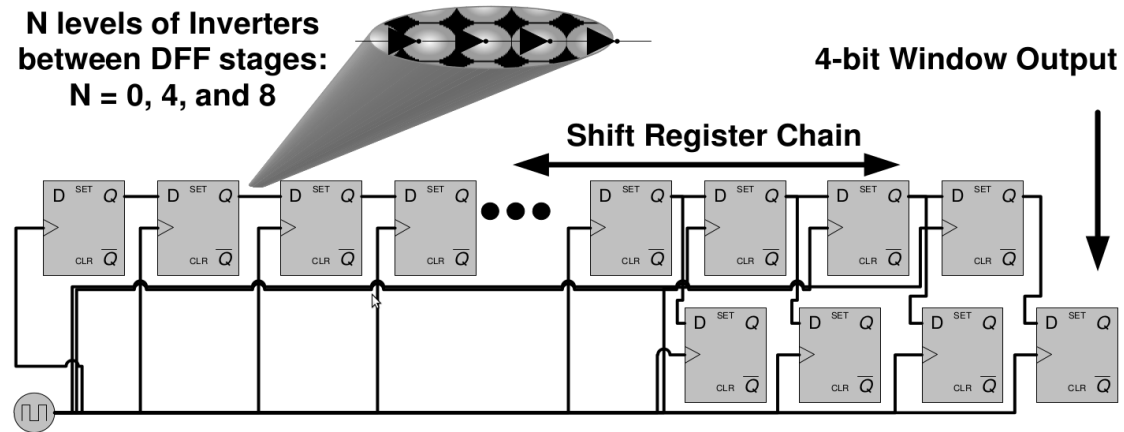


Figure 4.15: Flow chart for test procedure of SRAM

Single Event Latchup and PLL

⁴An n-bit Look-Up Table can encode any n-bit Boolean function by modeling such functions as truth tables

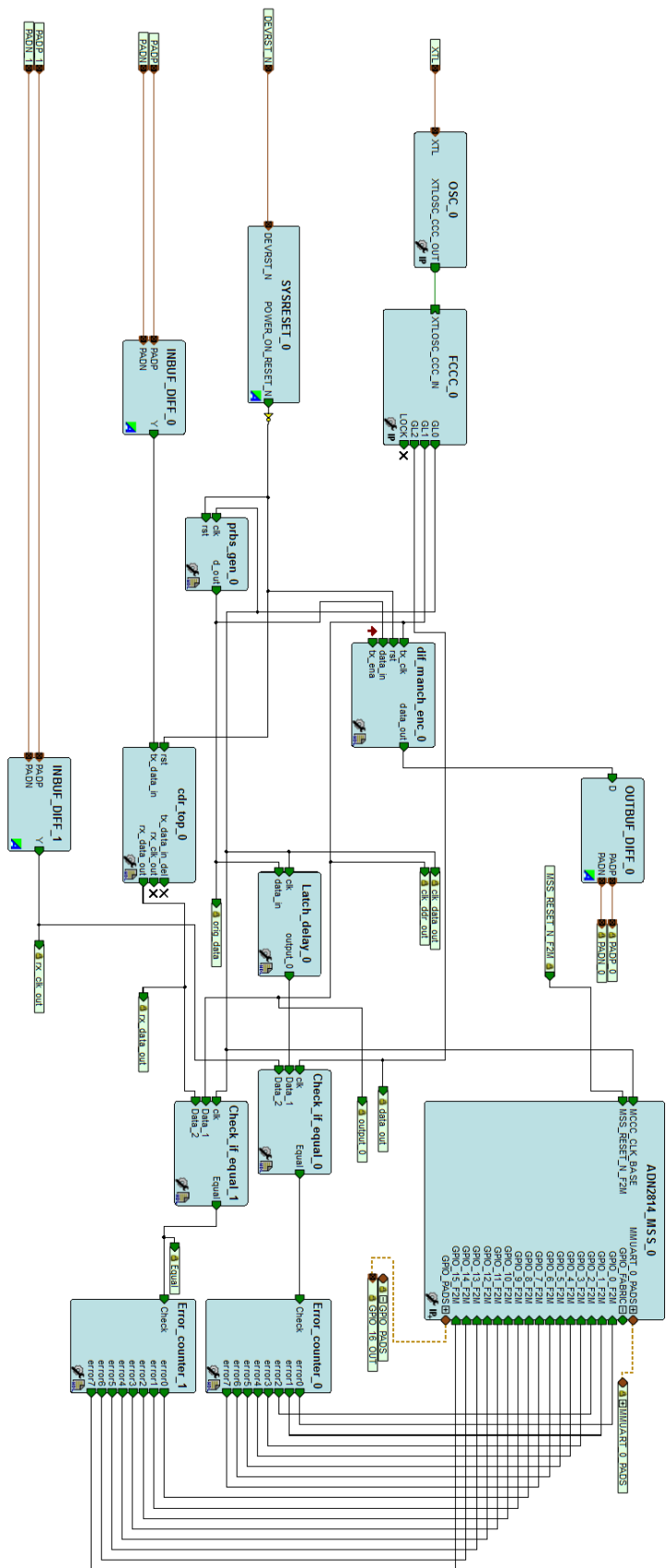


Figure 4.16: Smart Design for ADN2814

4.1.11 Software

To monitor the outputs and control the inputs and the supply voltage, a simple labVIEW program was made for each of the different PCBs. In these program time from start, current consumption and the status of the output signal (or the output voltage for the regulators) can be measured and monitored. Data is constantly saved to disk. In figure 4.17 you can see an example of a labVIEW program used for SN74AVC2T245.

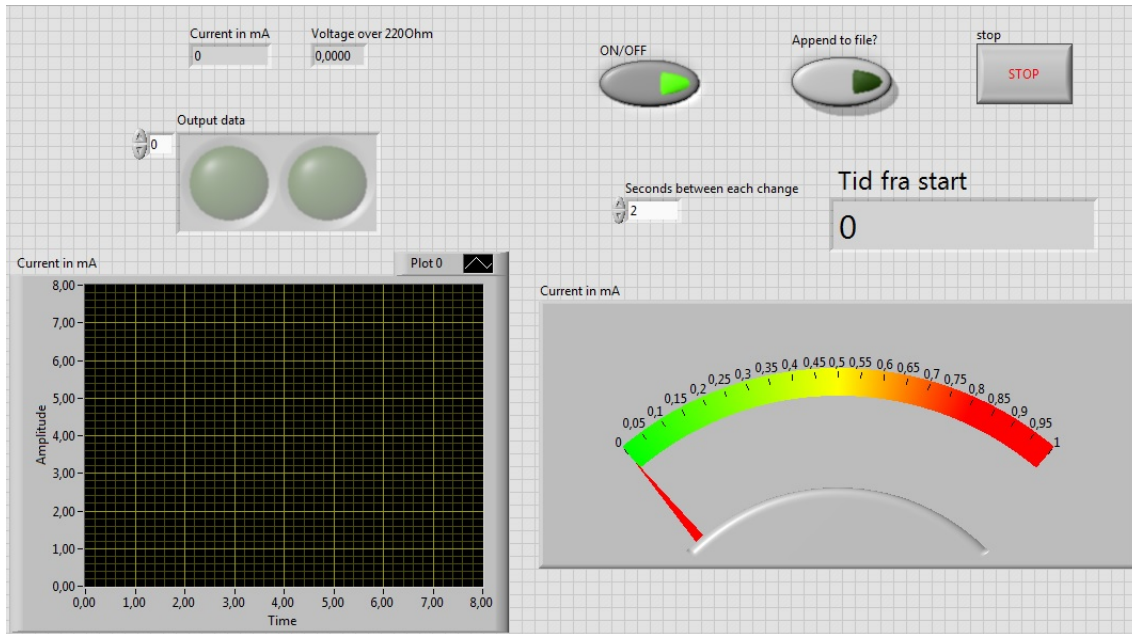


Figure 4.17: LabVIEW program for SN74AVC2T245

5 Testing at Oslo Cyclotron Laboratory (OCL)

5.1 About OCL

Oslo cyclotron Laboratory is located at the Department of physics at the University of Oslo, and was opened in 1978. The cyclotron is of the type MC-35 and was made by Scanditronix AB from Sweden. This is the only accelerator in Norway for ionized atoms used in basic research. The cyclotron can accelerate protons, deuteron, 3He and 4He , with energies and intensities as seen in the table 1 bellow. A drawing of the lab can be seen bellow in figure 5.1. The laboratory is divided in tree; the control room, the inner experimental hall and the outer experimental hall. The cyclotron is placed in the inner hall, and a beam is sent through pipes to the outer hall. There is vacuum inside the cyclotron and the pipes, so that you should not suffer energy loss from collision with air molecules. With magnet you are able to regulate the beam

to your desired pipe exit. There are also several cups put on the pipeline which makes it possible to block the beam. These can be used to stop the beam during an experiment, so you are able to go into the experimental area and do changes on your setup. When the cyclotron is running and the beam is on, you are not allowed to enter the inner experimental area.

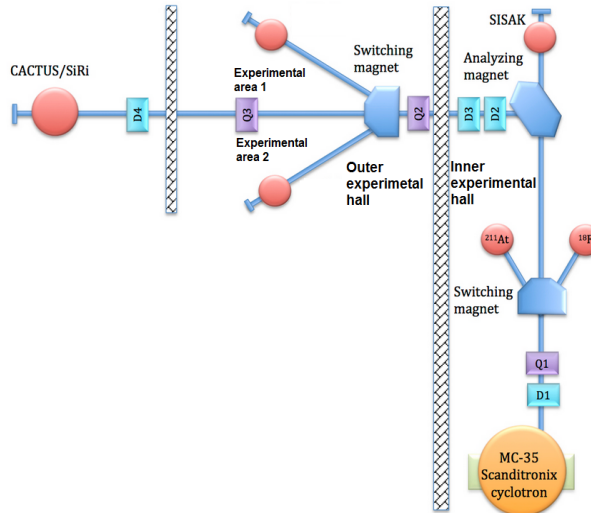


Figure 5.1: Out-lay of the OCL

| Ionized beam particle type | Energy(MeV) | Intensity(μA) |
|----------------------------|-------------|----------------------------|
| Proton | 2-35 | 100 |
| Deuteron | 4-18 | 100 |
| ^3He | 6-47 | 50 |
| ^4He | 8-35 | 50 |

Table 1: Ionized beam particle data table

5.2 Experiment setup and equipment

The experiment setup was placed in the outer experimental hall in experimental area 2. The experimental setup as well as the equipment used can be found in the figure and table bellow. The equipment was kept in close to the same height around 140-150cm (so that we wouldn't have to think about three dimensions). Beam exit was in a height of 141.5cm.

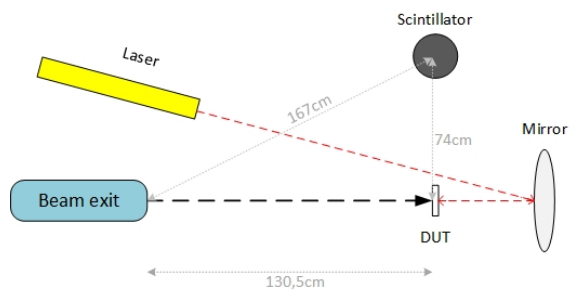


Figure 5.2: Experimental setup seen from above

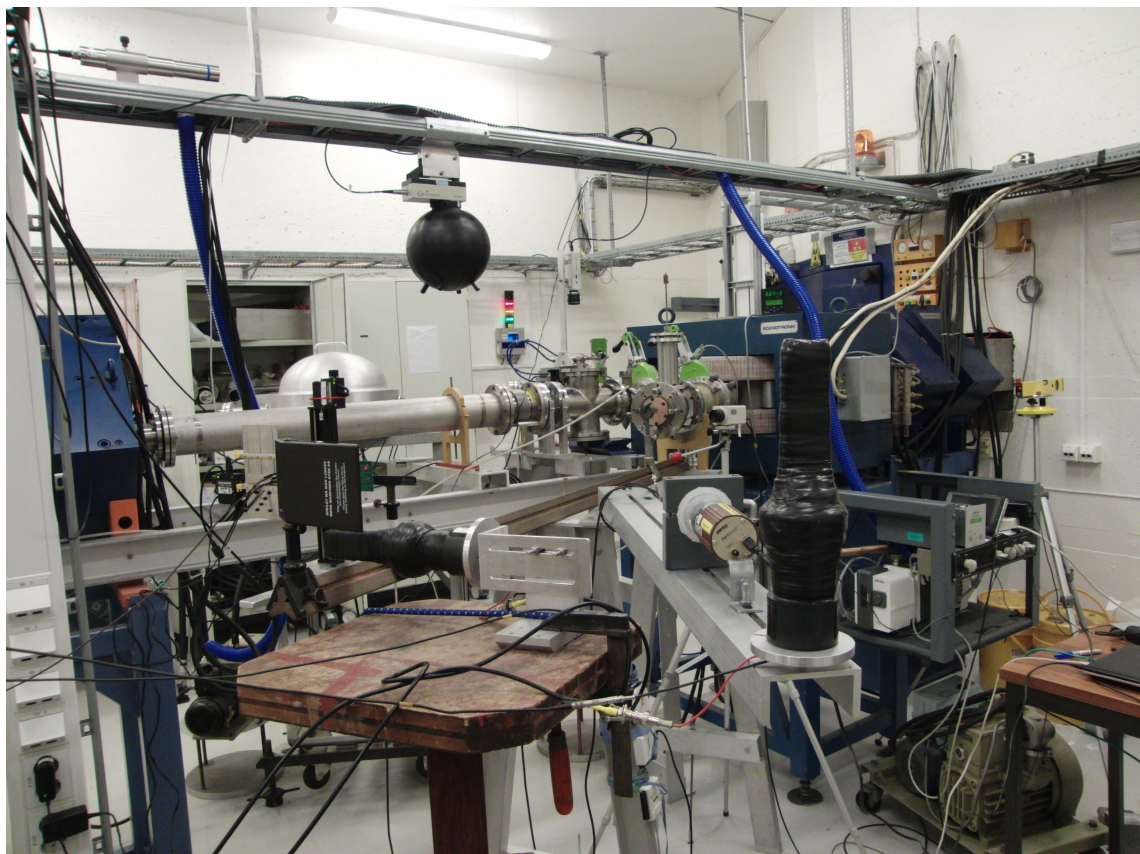


Figure 5.3: Picture of the experimental area

| Equipment | Explanation |
|------------------------|---|
| Scintillator | A plastic scintillator with photomultiplier. Was used to measure relative radiation. We had two of these, one that was placed right under Device Under Test (DUT) and one that was placed 75cm away from DUT. We only used the one 75cm away during the experiment. |
| High voltage regulator | Voltage for the photomultiplier. 800V was used |
| 8 test boards | TPS51200, MIC69302WU, SN74AVCB164245, SN74AVC2T245, QS3VH257, SY89831U, ADN2814 and MAX3748 |
| SRAM-board | A PCB board with 4 SRAM cells that was used to characterise the beam and to measure scintillator counts |
| SF2 starter kit | A starter kit board with the Smart Fusion 2(SF2) chip. |
| Computer | A VPN connection was set on a computer inside the experimental hall, so that we were able to control the experiment from the control room. The computer was running LabView to control the experiment. Data was also saved on the computer |
| USB DAQ | Data acquisition board form National Instruments(NI). Used to establish analog and digital connection to the test boards and send data to the computer. |
| Radiation film | A film that reacts when radiated with protons. Used to identify the beam. |
| Counting controller | A device that counts either rising or falling edges of a signal. |
| leveled laser | This was used to pinpoint the center of the beam. |
| Mirror | Used to reflect the laser beam to the backside of the test boards. |
| XY-controller | Connected to the computer so we can change the position of the test boards from outside the experimental area |

Table 2: Equipment used in the experiment

5.3 Measurement equipment and test boards

5.3.1 SRAM board

A SRAM memory chip is very sensitive to Single Event Effect (SEE), and can be used to measure relative radiation by constantly checking for SEU.

The method of detecting an Single Event Upset (SEU) in a SRAM is rather straight forward, as can be seen in the flow diagram of figure 5.4. There is an initial

startup phase where a known pattern is written to all the addresses in the SRAM. When the startup phase is done, the value from the first address is read back and compared to a known value by XORing the known value with the one read. If they are not equal a SEU has occurred, and a the XOR-function will go high and a 1 will be added to a SEU counter. The correct value is then written back to the address and the system moves on to the next address.

A checkerboard pattern, a pattern of alternating ones and zeros, is used when writing to the SRAM. To check for stuck bits, the bit pattern in the whole address space is inverted after each read.

From earlier experiment with the SRAM chip [18], the cross section(the probability that an incoming particle will induce an SEU) is known, and is found to be to be $1.14 \times 10^{-6} \text{ cm}^2$. By counting number of SEU during an experiment, we can by dividing on the cross section find how many particles that hits the chip. The SRAM board that we used consist of 4 SRAM chips, a flash based FPGA, connections and supporting electronics. The FPGA on the SRAM PCB is designed with RS485 two-way communication which makes it possible to edit firmware as well as sending data out. Through the experiment the SRAM PCB was connected with RS485 to Opal Kelly XEM3001 which gave us connection to a computer. On the computer we ran a LabVIEW program, that made us able to monitor data, as well as doing some settings. The SRAM board also had an optical input for scintillator counts, so we could by the use of this board also monitor scintillator counts.

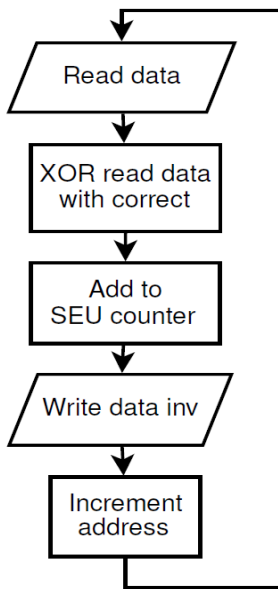


Figure 5.4: Flowchart for SEU detection

In figure 5.5 bellow you can see how the labVIEW program looked like. From here we can monitor SEU on all the 4 SRAM cells, see scintillator counts, reset counters, see time from start as well as other things. SRAM1-10 as you can see on the left side, is different SRAM-board, the board we used was SRAM6.

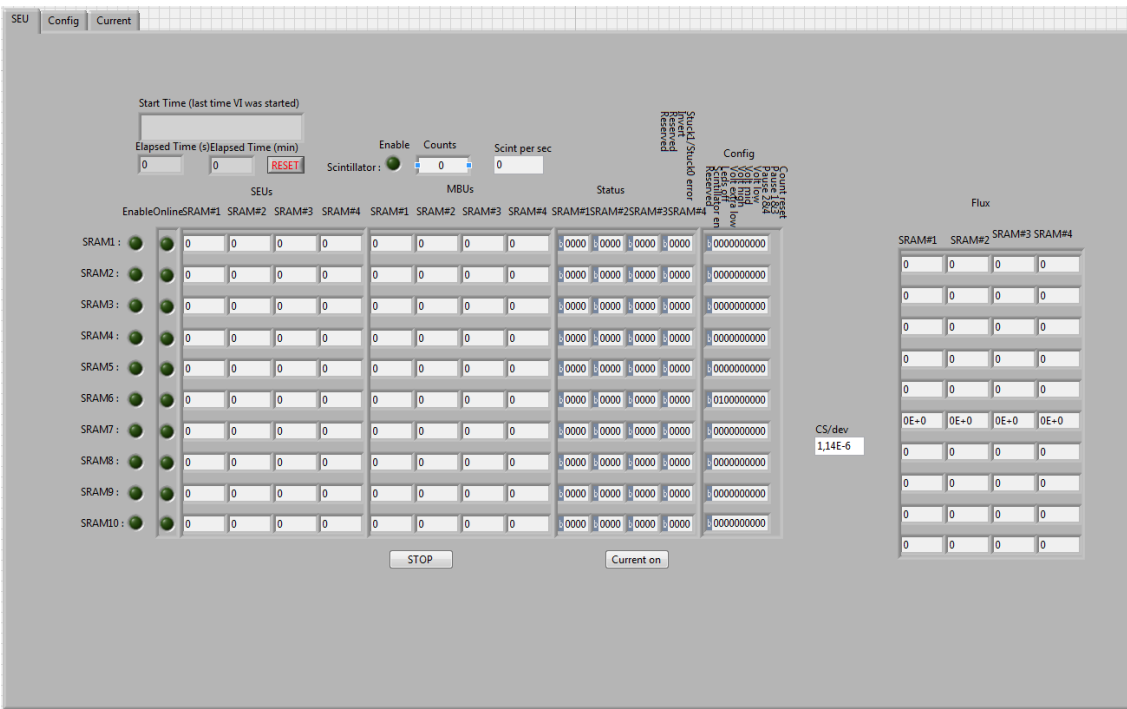


Figure 5.5: LabVIEW program for the SRAM

5.3.2 Scintillator counter

A scintillator is a material that gives out light when it is exposed to ionised radiation. A scintillator can be used as a stand alone equipment, but then only to detect that there are radiation, by seeing that it lights up. To get a more accurate measurement, we will need a PhotoMultiplier Tube (PM-tube). The PM-tube converts light pulses to current by an electron avalanche process. This process is very sensitive to radiation. [15] The pulses could be measured with the SRAM board or a counter of some kind, we used the SRAM board to measure scintillator counts during the experiments.

5.3.3 X-Y-positioning system

The X-Y-positioning system is a system that makes it possible to mount our PCBs and move them in X and Y direction. This could be controlled directly on the X-Y-system or through a labVIEW program on the computer. This was used when doing the beam profile as discussed in chapter 5.4.2, to be able to do changes on the position from the control room. In figure 5.6 you can see a picture of the front and back of the X-Y-positioning system.

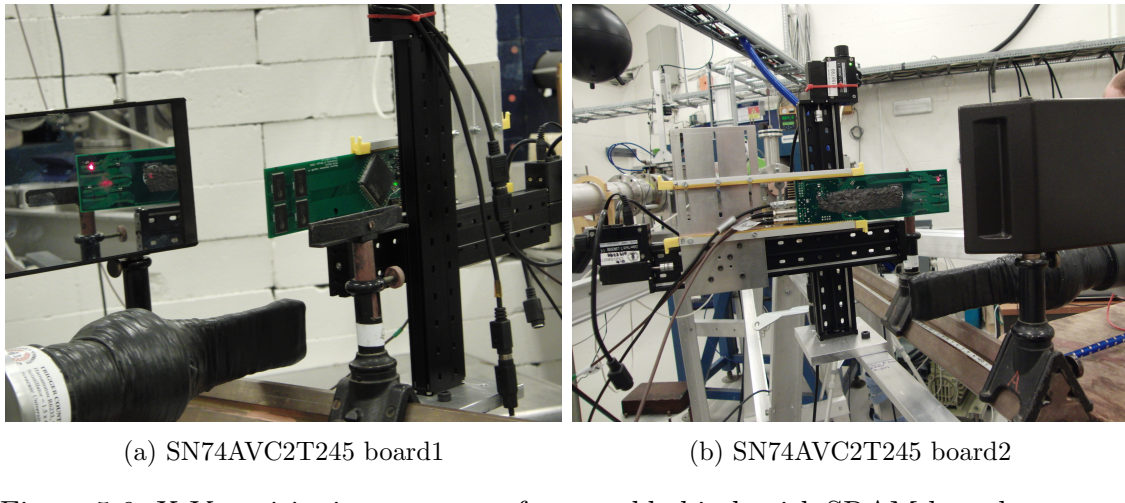


Figure 5.6: X-Y-positioning system upfront and behind, with SRAM-board mounted

5.4 Preparation and characterization of the beam

Before we could start testing of the PCB, the cyclotron had to be made ready for a proton beam and the magnet controlling the direction had to be put in the right position to get the beam out in experiment area 2.

5.4.1 Purpose of tests

The purpose of testing these board is to see if they are able to survive in a radiated area as we will find in the LHC, see section 1.1. To make sure that we know the limit of the ICs, the ICs was irradiated until a error occurred, current consumption drastically increased or the IC received a much higher dose than was required without error. Every IC that has been tested, are ICs that are going to be used in creation of the new RCU2 board.

5.4.2 Beam setup

When the beam was set, we could start the characterization of the beam. The first thing to do is to get an understanding of the beam, and see that it hits around the area that we expect at our test position 130.5 cm from beam exit. This was done by using radiation films that turns black when exposed to radiation. One of these was placed right in front of the beam exit and one in front of Device Under Test (DUT) area to see how the beam looks like at the two positions. This gave us a rough center position. A more precise calibration was done by the use of the SRAM board and the scintillator. By measuring the relation between scintillator counts on the scintillator which was in a locked position and SEU on the SRAM that was connected to the XY-position system(which made the SRAM freely to move), we were able to find a more precise position of the beam center by seeing which position gave us highest SEU counts compared to scintillator counts. When the beam center is found and everything works as it should, the laser was placed in a position so that the laser beam points to where we had found center of the beam to be. After that we could replace the SRAM board with the PCB that we were going to test. This had to be done every day at startup, before we could start the actual tests.

We were able to control the intensity(Current) of the beam freely from the control room inside the limitation of the beam (for protons that is up to 100 μA), but we kept us in the area between 100 pA to a few nA. This way the radiation dose to the test boards can be controlled. The beam intensity could be measured by putting a Faraday Cup(FC) in front of the beam. But the FC had to be removed when tests were running, since it will block the beam.

We were running 3 labVIEW programs at all time through the experiment, one for controlling the XY-position system, one for the SRAM board(to measure SEU and scintillator counts when calibrating and to get scintillator counts during the tests) and one program for each of the test boards. The SRAM and test board programs were constantly saving data on the disk.

6 Results and calculations from beam test at OCL

The radiation was done in 5 days divided in two periods 13.11.13-15.11.13 and 28.11.13-29.11.13. I had made two version of most of the boards, the exception is ADN2814 and MAX3748 which I only made one version of. The boards that where tested the first time are: *TPS51200₁, MIC69302WU₁, SN74AVCB164245₁, SN74AVC2T245₁, QS3VH257₁* and *SY89831U₁* tested in that order. The second time, we started with the two limiting amplifier IC, since those hadn't been tested before. So the order the PCB was tested the second period was: *ADN2814, MAX3748, SY89831U₂, TPS51200₂, MIC69302WU₂, SN74AVCB164245₂, SN74AVC2T245₂*. The first time at OCL we were given an beam of 28 MeV, but the second time the lab personnel manage only to produce a beam of 25MeV. When the beam gets out through the beam exit the energy will be reduced by crashing with air particles(21keV per cm), so at DUT area the beam was approx 25 MeV and 22 MeV.

The result is presented after type, so that the two boards of the same type is presented together.

6.1 Calibration process

As explained in chapter 5.4.2, we had to start by finding the center of the beam. In table 3 you can see the results from our calibration 15.11.2013. You can see that position x = -2,5 and y = -1 gives highest relation between SEU on the SRAM and scintillator counts. A total of 4 tests in that position was done and the average value gives us 0,0948. This value was used to calculate from scintillator counts to SEU. cross section(the probability that an incoming particle will induce an SEU) is known for the SRAM board. The cross section (CS) is given in equation 6.

$$CS = 1,14e - 6 \quad (6)$$

6.2 Test results

The tests was controlled and monitored through a LabVIEW program for each of the different IC. When testing ADN2814 and MAX3748 there was also needed a SF2 board to produce a input signal, and compare the input with the output signal. A complete result of the tests can be found in appendix 8. The point of this test was to see that these ICs would survive in a radiated area. The total dose of 10 years in the ALICE detector is estimated to be a 1-2 kRad, see section 1.1. If a IC survives

| Calibration test nr.: | x | y | Scint rel | SEU(SRAM) | SEU(SRAM)/sc |
|-----------------------|------|------|-----------|-----------|--------------|
| 1 | -0,8 | -1 | 27798 | 1463 | 5,26E-02 |
| 2 | -1,3 | -1 | 17721 | 1239 | 6,99E-02 |
| 3 | -1,8 | -1 | 12904 | 1203 | 9,32E-02 |
| 4 | -2,3 | -1 | 13361 | 1276 | 9,55E-02 |
| 5 | -2,8 | -1 | 12786 | 1238 | 9,68E-02 |
| 6 | -3,3 | -1 | 12342 | 1156 | 9,37E-02 |
| 7 | -2,5 | -1 | 11696 | 1223 | 1,05E-01 |
| 8 | -2,5 | -1,5 | 11027 | 1075 | 9,75E-02 |
| 9 | -2,5 | -2 | 11835 | 1063 | 8,98E-02 |
| 10 | -2,5 | -0,5 | 15593 | 1540 | 9,88E-02 |
| 11 | -2,5 | 0 | 12620 | 1034 | 8,19E-02 |
| 12 | -2,5 | -1 | 65280 | 5999 | 9,19E-02 |
| 13 | -2,5 | -1 | 52752 | 4803 | 9,10E-02 |
| 14 | -2,5 | -1 | 57229 | 5250 | 9,17E-02 |

Table 3: Calibration tests 15.11.2013

more than 10 times that, we can be quite sure that it will survive the radiation it will receive at CERN. In table 4 and 5 you can see how long each ICs has been exposed too radiation, the dose they have been received and if an error occurred.

| Device | Exposed time[s] | Dose[Rad] | Error |
|-----------------------------------|-----------------|-----------|-------|
| <i>TPS51200</i> | 2065 | 41800 | No |
| <i>MIC69302WU₁</i> | 2240 | 164000 | No |
| <i>SN74AVCB164245₁</i> | 967 | 65200 | No |
| <i>SN74AVC2T245₁</i> | 860 | 4600 | Yes |
| <i>QS3VH257₁</i> | 795 | 52800 | No |
| <i>SY89831₁</i> | 1251 | 93500 | No |

Table 4: Tests at OCL 15.nov 2013

| Device | Exposed time[s] | Dose[Rad] | |
|-----------------------------------|-----------------|-----------|-----|
| <i>ADN2814/run1</i> | 1273 | 20200 | Yes |
| <i>ADN2814/run2</i> | 2286 | 324900 | Yes |
| <i>MAX3748</i> | 2384 | 442200 | No |
| <i>TPS51200₂</i> | -* | -* | -* |
| <i>MIC69302WU₂</i> | 1385 | 383800 | No |
| <i>SN74AVCB164245₂</i> | 526 | 201400 | No |
| <i>SN74AVC2T245₂</i> | 478 | 161600 | No |
| <i>QS3VH257₂</i> | 264 | 110300 | No |
| <i>SY89831U₂</i> | 921 | 165800 | No |

* The board wouldn't work at test time

Table 5: Tests at OCL 27-28.nov 2013

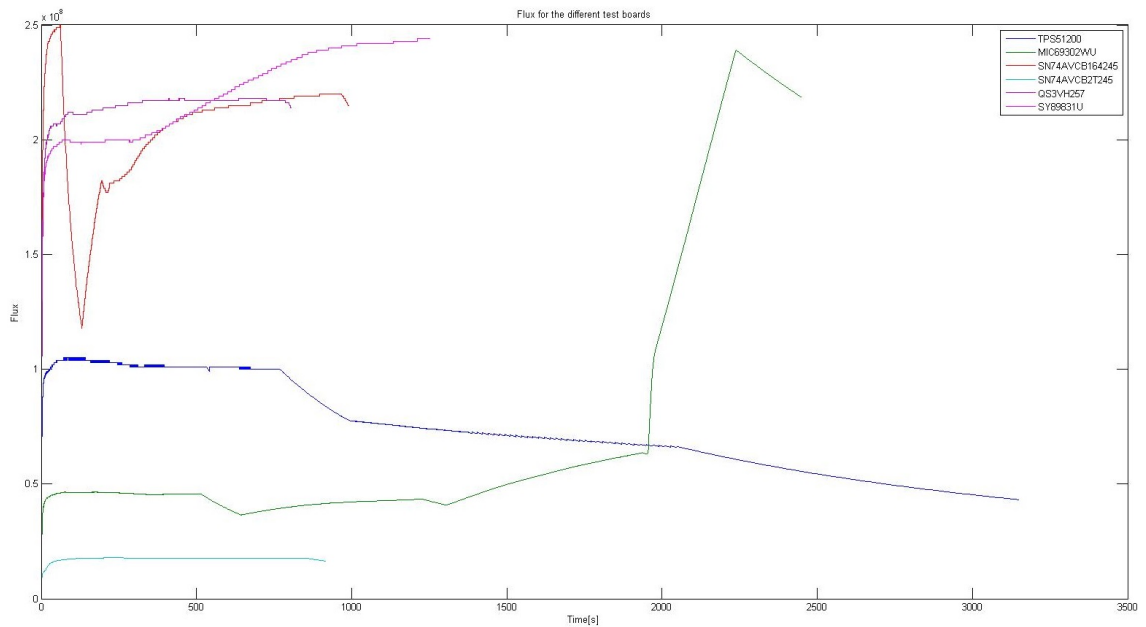


Figure 6.1: flux for each component radiated 15.11.2013

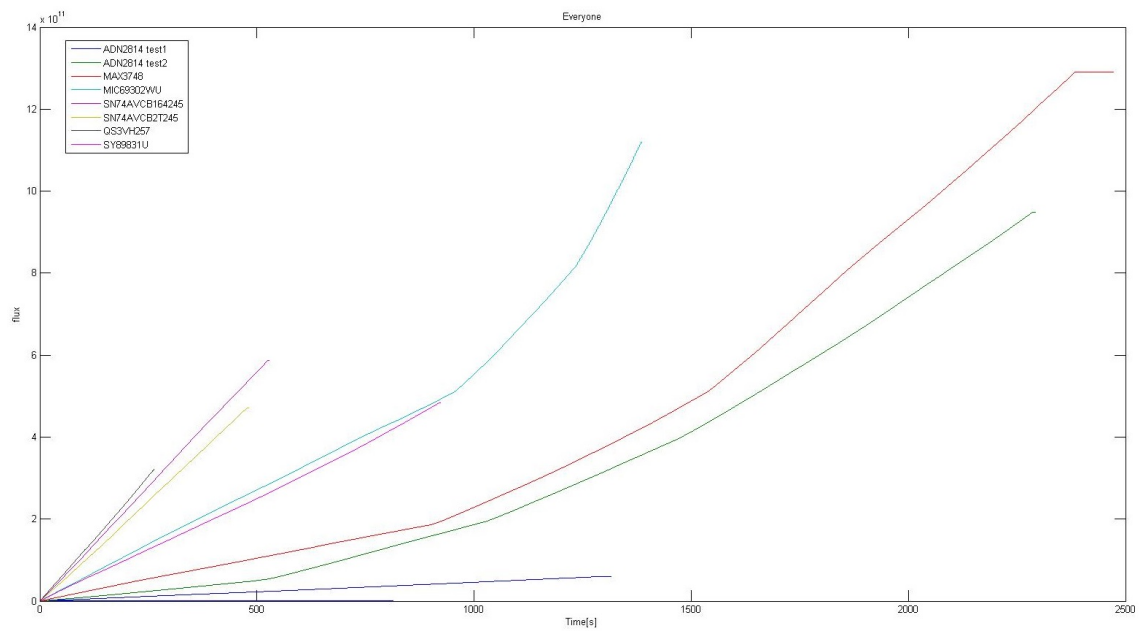


Figure 6.2: flux for each component radiated 15.11.2013

In figure 6.1 and 6.2 you can see graphs of flux vs time for the different test boards. The reason the graphs don't go as linear as one would expect, is that the beam sometimes stopped and had to restarted, and that we increased and decreased the intensities as we wanted.

6.2.1 TPS51200

This was the first board that was tested. The intensity was a little low on this test. To make the testing process faster the intensity was increased during the later experiments.

The IC worked after a dose of 40kRad, but we could see a little increase in current after a dose of 25 kRad. The output voltage is close to stable, a few mV up and down, but not noteworthy. Two PCBs of this type was tested, but only one worked when we was at OCL to do the testing.

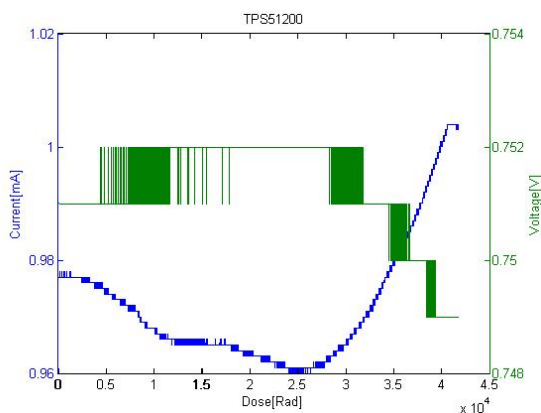
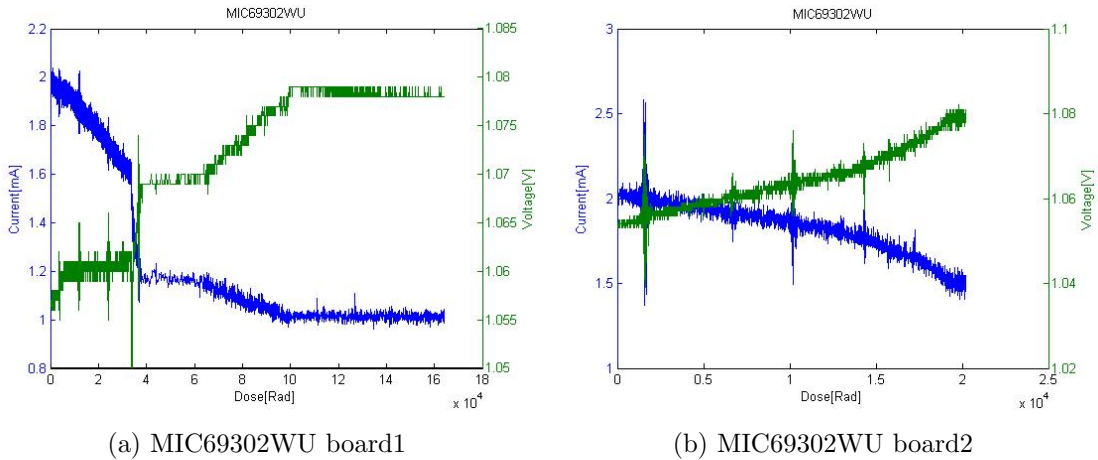


Figure 6.3: TPS51200 - Current/Voltage vs Dose

6.2.2 MIC69302WU

The first board was tested 15.11.13 and the second board was tested 28.11.13. During the test of the first board we increased the intensity of the beam quite allot, that can be seen from the flux graph, in figure 6.1.

This IC had an unexpected reaction to irradiation. You can see from both of the graphs that the current is decreasing and voltage is increasing, normally we would expect the opposite, or at least that the current would increase. As seen from the graph in figure 6.4 it starts quite early to decrease in current, but as you can see it also stabilize after a while. The output voltage is mostly stable, there were a increase of 2% on both of the tests.



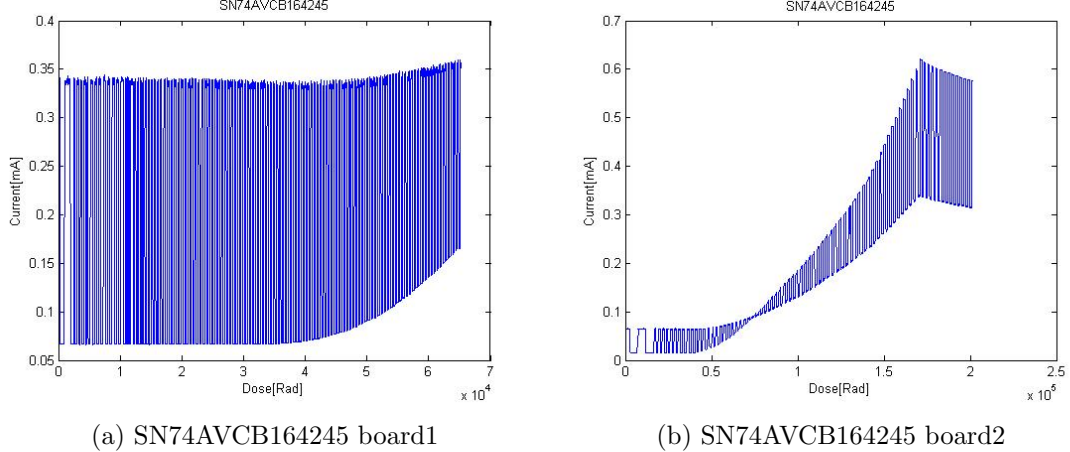
(a) MIC69302WU board1

(b) MIC69302WU board2

Figure 6.4: MIC69302WU - Current/Voltage vs Dose

6.2.3 SN74AVCB164245

It can be seen that the characteristics on the two test board are different, the reason for this is maybe because of different output load. The reason for the “jumps” in current is because the output is constantly changing from on to off, with a gap of 4 seconds. This chips is not effected by radiation before a dose of approx 40kRad. That is more than enough for the purposes we are going to use this for.



(a) SN74AVCB164245 board1

(b) SN74AVCB164245 board2

Figure 6.5: SN74AVC2T245 - Current vs Dose

6.2.4 SN74AVC2T245

Something went wrong on the first test. After 740 s and a dose of 98 Rad the chips output was stuck at 1. The reason for this is unknown, I fear that this might be defected before we started the test, since it gives a totally different characteristics than test board nr 2. The input was switching from high to low every 4 second. If

we look at the test results from board 2, the current goes unchanged up to 40 kRad, and that is more than enough.

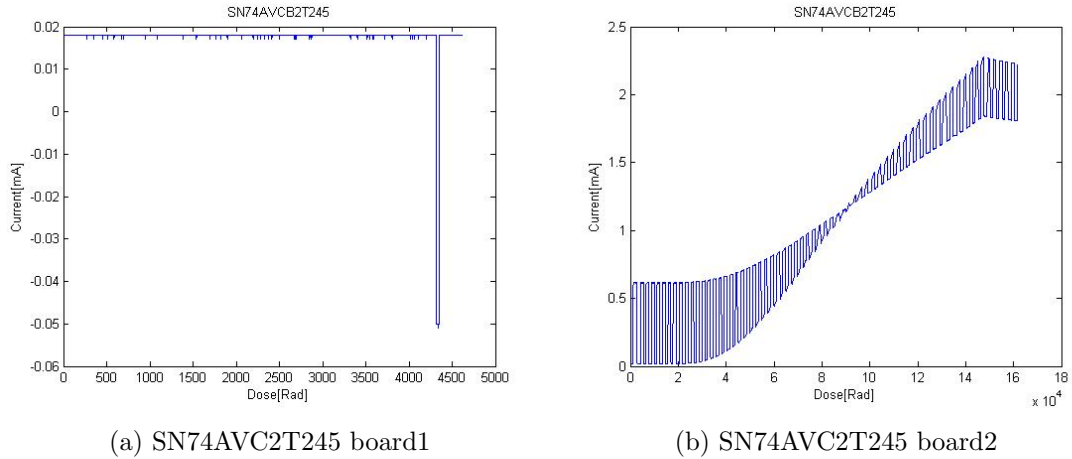


Figure 6.6: SN74AVC2T245 - Current vs Dose

6.2.5 QS3VH257

The select input was changed every 4 second and the inputs(I0A, I0B, I0C, I0D, I1A, I1B, I1C and I1D) was inverted every 18 second.

The two test boards worked fine through the tests. We see that we have small increase in current before 30 kRad, after that it increases quite allot. We couldn't see any errors on the output during the experiment, but it should probably not be exposed to more than 30 kRad.

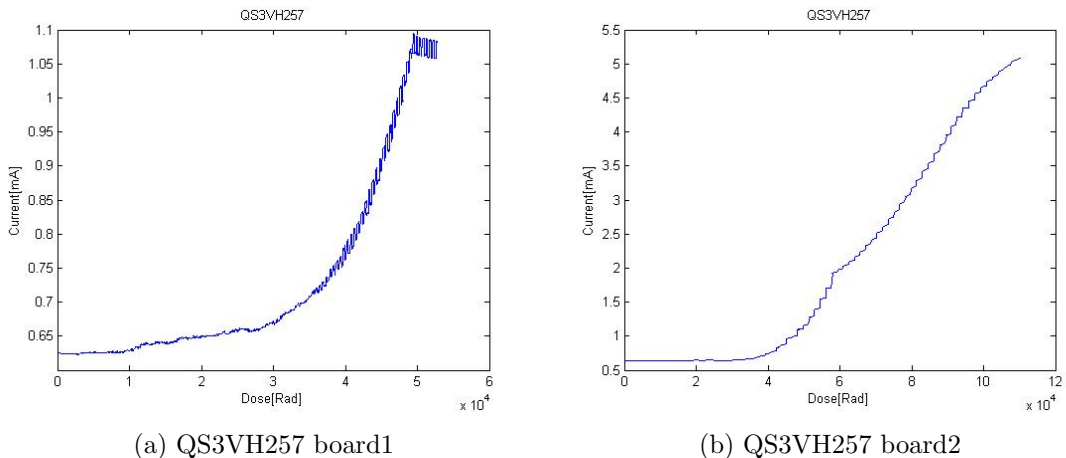


Figure 6.7: QS3VH257 - Current vs Dose

6.2.6 SY89831

This IC required a high current to work, and since the labVIEW DAQ device only delivers 5mA on the analog outputs, a combination of the modified MIC69302WU as described in section 4.1.2 and the 5V output on the DAQ was used. This gave us a output of 3.3 V and a current limit of 200 mA. Here a 20Ω resistor was used to measure current instead of a 220Ω resistor, this was to reduce the voltage drop over the resistor because of the high current consumption.

A difference in characteristics can also be seen here. This may be because two different footprint for the PCB was used, and therefore some difference can be seen. We see a small increase in current on both of the boards, but not noteworthy, compared to how much current this IC is using.

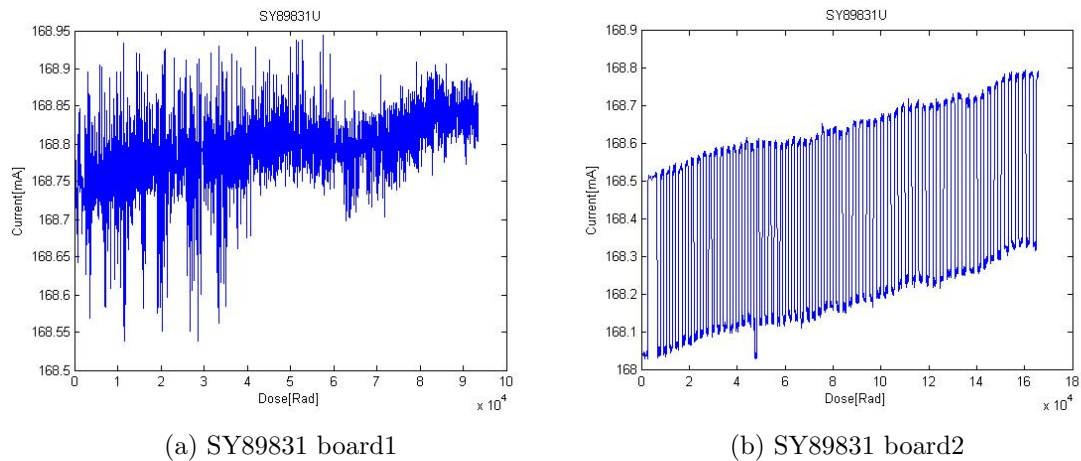


Figure 6.8: SY89831 - Current vs Dose

6.2.7 ADN2814

This IC is a little special and was hard to get a good test on. This is a clock and data return circuit, with a limiting amplifier. The SF2 board was used to code a clock and data into a differential Manchester signal, that was sent into the IC. Out of the IC we get a LVDS clock and LVDS Manchester signal. The Manchester coded data signal was decoded on SF2 board, so that we get out a clock and data. The data was tested by delaying the original data through a few D-latches, so that the original and returned data was close to synced. Then we could compare the original data with the one from the IC through a XOR-function. This function was triggered by a 80 Mhz clock from the SF2 board. If they aren't equal when the clock rises, a 1 will be added to a counter. The value of the counter was constantly sent through the UART of the SF2 board.

The way the clock was tested was a little harder process since the clock was so fast

(160 Mhz). This was solved, was by adding a third clock with the same frequency (160 Mhz) that was 90° of from the two others, when this goes high I called on the XOR-function, to see if the two other clocks are the same. if they are alike, nothing happens, if they are not the program adds 1 to a counter, which constantly writes its current value to a Universal Asynchronous Receiver/Transmitter (UART). The problem here is that for each time the SF2 board was programmed the clock was slightly different, that made either the clock out of sync or the data out of sync, so the code didn't always work as it should. This circuit also requires allot of current, therefore the same solution as for SY89831 was used, using MIC69302WU as a power supply and measure the current on that PCB.

The current didn't change before a dose of 200 kRad had been received, but we got a clock error at a dose of ~ 11 kRad, and a data error after a dose of ~ 8 kRad. How good this test really is, could be discussed, since we don't have any data on the clock and data, other than that the XOR-function failed. What really failed, and how much is impossible to know. It could be a slightly delay on a clock or the data, or maybe the clock just disappeared for a moment.

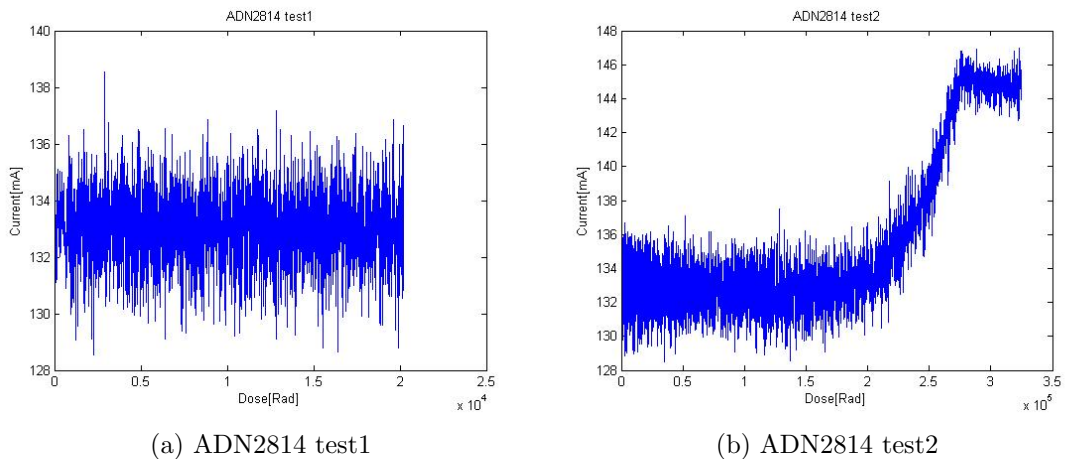


Figure 6.9: ADN2814 - Current vs Dose

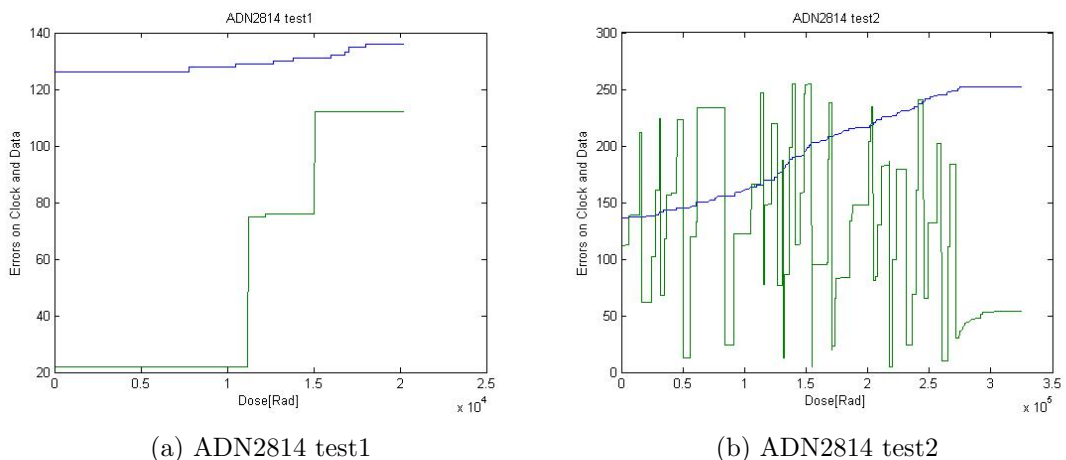


Figure 6.10: ADN2814 - Relative errors vs Dose

6.2.8 MAX3748

This circuit has the same purpose as ADN2814, the difference is that this one only return the limited Manchester coded signal, and no clock. The process for testing the data is the same as for the ADN2814. The decoding process return clock and data, but since they are related to another, a error on the clock would mean an error at the data. So by measuring data, we can be sure that there are no clock errors as well.

After a dose of over 400 kRad this chip still worked, and current consumption was stable through the hole irradiation process.

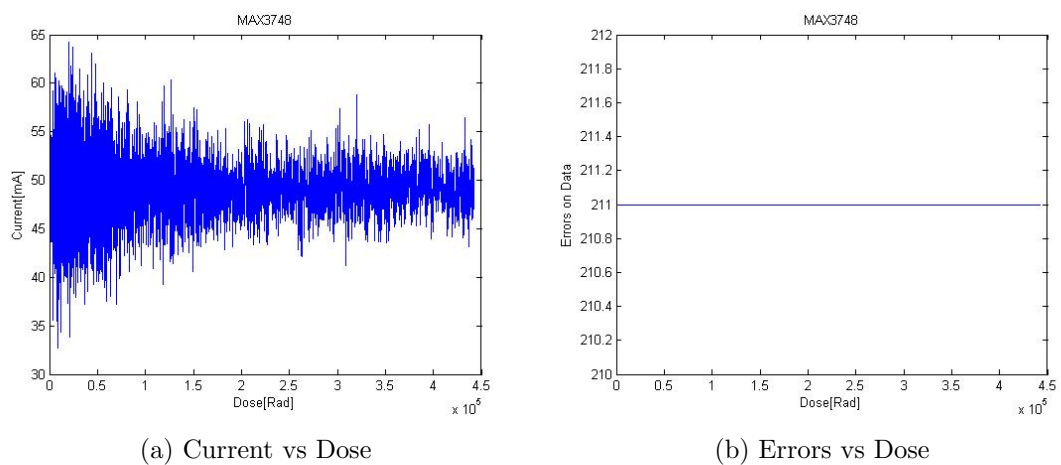


Figure 6.11: MAX3748

6.3 Calculation of dose

After a radiation test on one of the PCB, we knew the exposed time and scintillator counts. From the calibration we got the relation between scintillator counts and SEU on the SRAM, and the cross section for the SRAM is known. We start by calculating SEU from the conversion factor found in the calibration process, for 15.11.13 this was 0.0948 and for 28.11.13 this factor was 0.0473. Then we calculate the fluence at DUT as seen in equation 7, and by this we can calculate the flux, see equation 8. To calculate the dose from here we need to know some more factors. We run a simulation on a program called FLUKA. This program is used to simulate particles in different environment. We simulated a proton beam of 28MeV and 25MeV in air, and inserted the distance from BE(Beam exit). The results can be seen in table 6. Then we had enough information to calculate the dose. As seen from equation 9 we are able to find the Fluence at BE. And from there we can calculate the dose at DUT, see equation 10.

| Fluka simulation results 28MeV | |
|----------------------------------|-------------|
| Dose/primary particle at DUT[Gy] | 4,08E-10 |
| Primary particles at Beam exit | 1 |
| Primary particles at DUT | 0,1331 |
| Beam intensity reduction at DUT | 7,513148009 |

Table 6: FLUKA simulation with 28MeV proton beam

$$Fluence_{DUT} = \frac{SEU}{CS} \quad (7)$$

$$Flux = \frac{Fluence}{time} \quad (8)$$

$$Fluence_{BE} = \frac{fluence_{DUT}}{primary_particles_{DUT}} \quad (9)$$

$$Dose_{DUT}[Gy] = Fluence_{BE} \times \frac{Dose}{primary_particle_at_DUT} \quad (10)$$

$$1Rad = 100Gy \quad (11)$$

6.4 Discussion of the result

Most of the testing was done 15.nov and 28.nov. The other days was used to get familiar with the instruments and equipment that was being used, to prepare the setup and setting up the beam. There are almost impossible to get the same beam two days at a row. Each day of testing is therefore different from each other. Since the testing was conducted in two periods and a total of 4 test days, there are allot of uncertainties regarding the beam. And that is also why we had to do calibration each day at start-up.

When we were going to measure the intensity at the beam exit, we placed a Faraday cup in front of the beam, and connected it to a amperemeter on the control panel, but since the current is so small, the measuring instrument will be affected by air currents, and there are also allot of uncertainties in the instruments. Therefore we only used the Faraday cup and the amperemeter, to get a rough estimate of the actual intensity.

The are also some uncertainties regarding the DAQ device form NI. When measuring digital signal, we don't know if it goes from 0 V to 3.3 V as we would expect. Maybe in reality the low voltage is actually 0.4 V and high voltage is actually 2.8 V. If this is the case, it could be a problem with using this in our design.

As said before in 5.4.2, if a component survives 10 times more than what it will receive in a period of 10 years in ALICE, that is 1-2 kRad, than it can be used in the design of RCU2. Having that in mind, I would say that every component tested would have a green flag even though we had some errors when testing SN74AVC2T245 and ADN2814. Since the result after testing board two of SN74AVC2T245 was positive we can assume that something was wrong with the first board. When it comes to ADN2814, it would be nice to have more time in the lab to test this even more, since the test done gave us so unclear results. If a better test would be made, I'm sure that this would perform much better.

7 Conclusion

8 Appendix

8.1 datasheets

| Calibration test nr.: | x | y | Scint rel | SEU(SRAM) | SEU(SRAM)/sc |
|-----------------------|------|------|-----------|-----------|--------------|
| 1 | 0 | 0 | 23813 | 1971 | 8,28E-02 |
| 2 | 0 | -0,5 | 37930 | 3867 | 1,02E-01 |
| 3 | 0 | -1 | 27527 | 2817 | 1,02E-01 |
| 4 | 0 | -1,5 | 34413 | 3360 | 9,76E-02 |
| 5 | 0 | -2 | 32713 | 2763 | 8,45E-02 |
| 6 | 0,5 | 0 | 38753 | 2709 | 6,99E-02 |
| 7 | -0,5 | 0 | 23420 | 2483 | 1,06E-01 |
| 8 | -1 | 0 | 20611 | 2232 | 1,08E-01 |
| 9 | -1,5 | 0 | 21014 | 2410 | 1,15E-01 |
| 10 | -1,5 | 0 | 20676 | 2260 | 1,09E-01 |
| 11 | -2 | 0 | 35787 | 3776 | 1,06E-01 |
| 12 | -2,5 | 0 | 27847 | 2512 | 9,02E-02 |

Table 7: Calibration tests 14.11.2013

| Calibration test nr.: | x | y | Scint rel | SEU(SRAM) | SEU(SRAM)/ sc |
|-----------------------|------|------|-----------|-----------|---------------|
| 1 | -0,8 | -1 | 27798 | 1463 | 5,26E-02 |
| 2 | -1,3 | -1 | 17721 | 1239 | 6,99E-02 |
| 3 | -1,8 | -1 | 12904 | 1203 | 9,32E-02 |
| 4 | -2,3 | -1 | 13361 | 1276 | 9,55E-02 |
| 5 | -2,8 | -1 | 12786 | 1238 | 9,68E-02 |
| 6 | -3,3 | -1 | 12342 | 1156 | 9,37E-02 |
| 7 | -2,5 | -1 | 11696 | 1223 | 1,05E-01 |
| 8 | -2,5 | -1,5 | 11027 | 1075 | 9,75E-02 |
| 9 | -2,5 | -2 | 11835 | 1063 | 8,98E-02 |
| 10 | -2,5 | -0,5 | 15593 | 1540 | 9,88E-02 |
| 11 | -2,5 | 0 | 12620 | 1034 | 8,19E-02 |
| 12 | -2,5 | -1 | 65280 | 5999 | 9,19E-02 |
| 13 | -2,5 | -1 | 52752 | 4803 | 9,10E-02 |
| 14 | -2,5 | -1 | 57229 | 5250 | 9,17E-02 |

Table 8: Calibration tests 15.11.2013

| Fluka simulation results 28MeV | |
|----------------------------------|-------------|
| Dose/primary particle at DUT[Gy] | 4,08E-10 |
| Primary particles at Beam exit | 1 |
| Primary particles at DUT | 0,1331 |
| Beam intensity reduction at DUT | 7,513148009 |

Table 9: FLUKA simulation with 28MeV proton beam

| Fluka simulation results 25MeV | |
|--|------------|
| <i>Dose primary particle at DUT</i> [Gy] | 2,94E-10 |
| Primary particles at Beam exit | 1 |
| Primary particles at DUT | 8,57E-02 |
| Beam intensity reduction at DUT | 11,6713352 |

Table 10: FLUKA simulation with 25MeV proton beam

References

- [1] K. Aamodt, A. Abrahantes Quintana, R. Achenbach, S. Acounis, D. Adamova, C. Adler, and the rest of the ALICE Collaboration. The ALICE experiment at the CERN LHC. *JOURNAL OF INSTRUMENTATION*, 3, AUG 2008.
- [2] V.V. Balashov. *Interaction of particles and Radiation with Matter*. Springer-Verlag, 1997.
- [3] R.C. Baumann. Radiation-induced soft errors in advanced semiconductor technologies. *Device and Materials Reliability, IEEE Transactions on*, 5(3):305–316, Sept 2005.
- [4] Melanie Berg. Field programmable gate array (fpga) single event effect (see) radiation testing. February 2012.
- [5] National Instruments Corporation. User guide and specifications ni usb-6008/6009, April 2014. <http://www.ni.com/pdf/manuals/371303m.pdf>.
- [6] F. Faccio. Alice information site. <http://aliceinfo.cern.ch/>.
- [7] F. Faccio. Radiation effects in the electronics for cms. http://lhcb-elec.web.cern.ch/lhcb-elec/papers/radiation_tutorial.pdf.
- [8] Thomas Granlund and Nils Olsson. *A Comparative Study Between Proton and Neutron Induced SEU in SRAMs*, 53(4). 2006.
- [9] Texas Instruments. Tps51200 - sink/source ddr termination regulator, February 2008. <http://www.ti.com/lit/ds/slus812/slus812.pdf>.
- [10] Glenn F. Knoll. *Radiation Detector and Measurement*. John Wiley and Sons, 3 edition edition, 2000.
- [11] David M. Harris Neil H. E. Weste. *CMOS VLSI Design - A Circuit and System Perspective*. Addison-Wesley, 4 edition edition, 2011.
- [12] Ketil Røed. Irradiation tests of altera sram-based fpgas. Master’s thesis, Norway, 2004.
- [13] Ketil Røed. *Single Event Upsets in SRAM FPGA based readout electronics for the Time Projection Chamber in the ALICE experiment*. PhD thesis, Norway, 2009.

- [14] Bjørn Halvor Straume. Strålingstester og utvikling av bestrålingsposedyre for alice tpc-elektronikken. Master's thesis, Norway.
- [15] Tor F. Thorsteinsen. *Kompendium i Strålingsfysikk - FYS231/233*. University of Bergen, Bergen, 1995.
- [16] F.B McLean T.R Oldham. Total ionizing dose effects in mos oxides and devices. *IEEE TRANSACTIONS ON NUCLEAR SCIENCE*, 2003.
- [17] Georgios Karolos Tsiledakis. *Scale Dependence of Mean Transverse Momentum Fluctuations at Top SPS Energy measured by the CERES experiment and studies of gas properties for the ALICE experiment*. PhD thesis. Technische Universitat Darmstadt, Darmstadt, 2006.
- [18] Arild Velure. Design, implementation and testing of sram based neutron detectors. Master's thesis, Norway.